

1 Technical Note: Preventing CO<sub>2</sub> overestimation from mercuric or  
2 copper (II) chloride preservation of dissolved greenhouse gases in  
3 freshwater samples

4  
5 François Clayer<sup>1\*</sup>, Jan Erik Thrane<sup>1</sup>, Kuria Ndungu<sup>1</sup>, Andrew King<sup>1</sup>, Peter Dörsch<sup>2</sup>, Thomas Rohrlack<sup>2</sup>

6  
7 <sup>1</sup>Norwegian Institute for Water Research (NIVA), Økernveien 94, 0579 Oslo, Norway

8  
9 <sup>2</sup>Faculty of Environmental Sciences and Natural Resource Management, Norwegian University of  
10 Life Sciences, PO Box 5003, 1432 Ås, Norway

11  
12 \*Corresponding author(s): François Clayer ([francois.clayer@niva.no](mailto:francois.clayer@niva.no))

13  
14 **Abstract**

15 The determination of dissolved gases (O<sub>2</sub>, CO<sub>2</sub>, CH<sub>4</sub>, N<sub>2</sub>O, N<sub>2</sub>) in surface waters allows to estimate  
16 biological processes and greenhouse gas fluxes in aquatic ecosystems. Mercuric chloride (HgCl<sub>2</sub>) has  
17 been widely used to preserve water samples prior to gas analysis. However, alternates are needed  
18 because of the environmental impacts and prohibition of mercury. HgCl<sub>2</sub> is a weak acid and interferes  
19 with dissolved organic carbon (DOC). Hence, we tested the effect of HgCl<sub>2</sub> and two substitutes  
20 (copper (II) chloride – CuCl<sub>2</sub> and silver nitrate – AgNO<sub>3</sub>), as well as storage time (24h to 3 months)  
21 on the determination of dissolved gases in low ionic strength and high DOC water from a typical  
22 boreal lake. Furthermore, we investigated and predicted the effect of HgCl<sub>2</sub> on CO<sub>2</sub> concentrations in  
23 periodic samples from another lake experiencing pH variations (5.4–7.3) related to *in situ*  
24 photosynthesis. Samples fixed with inhibitors generally showed negligible O<sub>2</sub> consumption. However,  
25 effective preservation of dissolved CO<sub>2</sub>, CH<sub>4</sub> and N<sub>2</sub>O for up to three months prior to dissolved gas  
26 analysis, was only achieved with AgNO<sub>3</sub>. In contrast, HgCl<sub>2</sub> and CuCl<sub>2</sub> caused an initial increase in  
27 CO<sub>2</sub> and N<sub>2</sub>O from 24h to 3 weeks followed by a decrease from 3 weeks to 3 months. The CO<sub>2</sub>  
28 overestimation, caused by HgCl<sub>2</sub>-acidification and shift in the carbonate equilibrium, can be  
29 calculated from predictions of chemical speciation. Errors due to CO<sub>2</sub> overestimation in HgCl<sub>2</sub>-  
30 preserved water, sampled from low ionic strength and high DOC freshwater that are common in the  
31 northern hemisphere, could lead to an overestimation of the CO<sub>2</sub> diffusion efflux by a factor of >20  
32 over a month, or a factor of 2 over the ice-free season. The use of HgCl<sub>2</sub> and CuCl<sub>2</sub> for freshwater  
33 preservation should therefore be discontinued. Further testing of AgNO<sub>3</sub> preservation should be  
34 performed under a large range of freshwater chemical characteristics.

CO<sub>2</sub> overestimation from HgCl<sub>2</sub> fixation – Clayer et al.

35

36 **Key-words:** lake, greenhouse gases, water sample preservation, mercuric chloride, metal toxicity,  
37 carbon dioxide

38 **Running title:** CO<sub>2</sub> overestimation from HgCl<sub>2</sub> fixation

## 39 1 Introduction

40

41 The determination of dissolved gases by gas chromatography from water samples collected in the  
42 field allows the estimation of biological processes in aquatic ecosystems such as photosynthesis and  
43 oxic respiration (O<sub>2</sub>, CO<sub>2</sub>), denitrification (N<sub>2</sub>, N<sub>2</sub>O) and methanogenesis (CH<sub>4</sub>). This technique is also  
44 useful to test the calibration of *in-situ* sensors in long term deployment. However, the accuracy of this  
45 approach largely depends on the effectiveness of sample fixation. In fact, the partial pressure of the  
46 dissolved gases will continue to evolve in the water sample from the time of collection to the time of  
47 analysis unless biological activity is prevented. This is an issue when field sites are far from  
48 laboratory facilities, and when samples need to be stored until the end of the field season for more  
49 efficient processing in large batches. Hence, before using a given ~~bioicide-chemical~~ to preserve water  
50 samples, it must be ensured that it is efficient in inhibiting biological activity without changing the  
51 sample's chemistry.

52 Mercuric (II) chloride (HgCl<sub>2</sub>) has been widely used as an inhibitor of the above-mentioned biological  
53 processes to preserve water samples for the determination of dissolved CO<sub>2</sub> in seawaters (e.g.  
54 Dickson, Sabine & Christian, 2007) and several dissolved gases in natural and artificial freshwater  
55 bodies (e.g. O<sub>2</sub>, CO<sub>2</sub>, CH<sub>4</sub>, N<sub>2</sub> and/or N<sub>2</sub>O; Guérin et al., 2006; Hessen et al., 2017; Hilgert et al.,  
56 2019; Okuku et al., 2019; Schubert et al., 2012; Xiao et al., 2014; Yan et al., 2018; Yang et al., 2015)  
57 because it ~~is extremely toxic~~proved effective at very low concentrations compared to other reagents  
58 (e.g. Horvatić & Peršić, 2007; Hassen *et al.*, 1998). Worldwide efforts have sought to reduce the use  
59 of mercury because it is considered toxic to the environment and exposure can severely affect human  
60 health (Chen et al., 2018). Therefore, alternative preservation techniques to HgCl<sub>2</sub> ~~amendment~~  
61 treatment have been tested for dissolved inorganic carbon (DIC) and δ<sup>13</sup>C-DIC such as acidification  
62 with phosphoric acid (Taipale & Sonninen, 2009) or a combination of filtration and exposure to  
63 benzalkonium chloride or sodium chloride (Takahashi *et al.*, 2019). ~~At least two studies, one also~~  
64 ~~including dissolved organic carbon (DOC) and δ<sup>13</sup>C-DOC, Previous studies~~ showed that simple  
65 filtration (and cooling), fixation (precipitation) or acidification were effective in preserving water  
66 samples (Wilson, Munizzi & Erhardt, 2020). ~~Another solution~~An alternative to using preservatives is  
67 to collect in-situ water samples, is to sample~~extract~~ the headspace ~~out~~ in the field, and ~~bring back gas~~  
68 ~~samples~~analyze the headspace in a laboratory (e.g., Cole et al., 1994; Karlsson et al., 2013; Kling et  
69 al., 1991). However, these techniques were not tested for the simultaneous determination of several  
70 dissolved gases, including CH<sub>4</sub> which is subject to rapid degassing during handling or storage if  
71 samples are not preserved because of its low solubility in water (Duan & Mao, 2006). In addition,  
72 some of the existing alternatives, such as filtration or field headspace equilibration, are difficult to  
73 operate in remote areas in the field under harsh weather conditions and prone to potential ambient air  
74 contamination. Solutions for water sample preservation should therefore involve a minimum of

CO<sub>2</sub> overestimation from HgCl<sub>2</sub> fixation – Clayer et al.

75 manipulation steps in the field to avoid gas exchange with ambient air. ~~Bioicide-Preservative~~  
76 amendments into sealed water bottles appears as one of the most efficient methods. Copper(II)  
77 chloride (CuCl<sub>2</sub>) and silver nitrate (AgNO<sub>3</sub>), the most toxic form of silver, are relevant alternatives to  
78 HgCl<sub>2</sub> given their known toxicity (e.g., Ratte 2009; Amorim and Scott-Fordsmand 2012) and wide  
79 application in water treatments and water purification (Larrañaga et al., 2016; Nowack et al., 2011;  
80 NPIRS, 2023; Ullmann et al., 1985). Nevertheless, the efficiency of these alternative ~~bioicides~~  
81 ~~preservatives~~ has never been tested for dissolved gas samples preservation.

82 The addition of HgCl<sub>2</sub> to water is known to produce hydrochloric acid through hydrolysis (Ciavatta &  
83 Grimaldi, 1968) and to form complexes with many environmental ligands, both inorganic (Powell *et*  
84 *al.*, 2004) and organic (Tipping, 2007; Foti *et al.*, 2009; Liang *et al.*, 2019; Chen *et al.*, 2017). The  
85 complexation of Hg<sup>+</sup> with the carboxyl or thiol groups of DOC in oxic environments could further  
86 increase the concentration of H<sup>+</sup> (Khawaja et al., 2006; Skyllberg, 2008). This acidification can be an  
87 issue in poorly buffered water (low ionic strength) with high concentration of DOC where a shift in  
88 the pH and carbonate equilibrium can be induced. In that case, the estimated CO<sub>2</sub> concentration would  
89 be higher after HgCl<sub>2</sub> fixation than the *in situ* concentration, and if the shift in pH is not accounted for,  
90 can result in an overestimation of dissolved CO<sub>2</sub> and bicarbonate concentrations. A similar  
91 acidification effect is also expected with CuCl<sub>2</sub> ~~amendments-treatments~~ (Rippner et al., 2021), but not  
92 for AgNO<sub>3</sub> ~~amendments-treatments~~. Such effects would not be expected in marine water due to the  
93 high ionic strength of the water (Chou *et al.*, 2016) or freshwater with low pH (<5.5) under which  
94 conditions nearly all dissolved inorganic carbon is CO<sub>2</sub> (Stumm & Morgan, 1981). Thus, there are  
95 clear limits of the application of HgCl<sub>2</sub>, and possibly CuCl<sub>2</sub>, for freshwater sample preservation given  
96 its risk of leading to overestimation of CO<sub>2</sub> and bicarbonate concentrations, in addition to exposing  
97 field workers to the risks of its high toxicity.

98  
99 Here we combine data from laboratory experiments (i) and field work (ii) to illustrate risks of mis-  
100 estimation of dissolved gas concentrations in freshwaters with some preservatives and provide  
101 recommendation for best practices in the field. First, we (i) performed some short-term and long-term  
102 incubations of water from a typical heterotrophic unproductive boreal lake with circumneutral pH,  
103 low ionic strength (poor buffering capacity) and high DOC concentration to test the effect of storage  
104 time and different preservative ~~amendments-treatments~~ on the determination of five dissolved gases  
105 (O<sub>2</sub>, CO<sub>2</sub>, CH<sub>4</sub>, N<sub>2</sub> and N<sub>2</sub>O) by headspace equilibration and gas chromatography. The preservatives  
106 were mercuric chloride (HgCl<sub>2</sub>) and two alternative inhibitors, chosen for their wide and effective  
107 application in water treatments and water purification (copper (II) chloride – CuCl<sub>2</sub> and silver nitrate –  
108 AgNO<sub>3</sub>; Xu & Imlay, 2012; Rai, Gaur & Kumar, 1981). Unamended water samples, where only  
109 ultrapure water was added, were also included for comparison. In addition, we (ii) analysed dissolved

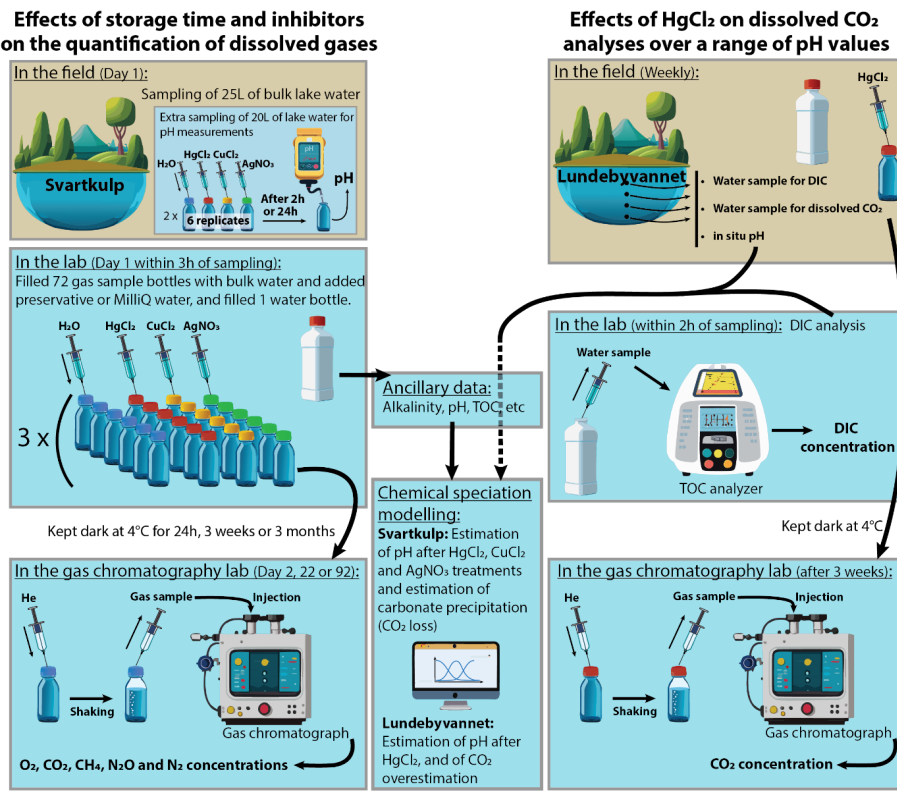
110 CO<sub>2</sub> concentration data obtained from a typical productive boreal lake using two independent  
 111 methods, one by gas chromatography following HgCl<sub>2</sub> fixation, and one through dissolved inorganic  
 112 carbon determination without fixation. We show that the overestimation of dissolved CO<sub>2</sub>  
 113 concentrations caused by HgCl<sub>2</sub> fixation can be predicted based on chemical equilibria.

114

115 **2. Methods**

116 The detailed experimental procedures for investigating (i) the effects of storage time and different  
 117 inhibitors on dissolved gas concentrations as well as (ii) the effects of HgCl<sub>2</sub> on dissolved CO<sub>2</sub>  
 118 analyses over a range of pH values are summarized in Fig. 1 and described below.

Formatted: Font: Not Bold  
 Formatted: Subscript  
 Formatted: Subscript



119

120 **Fig. 1.** Overview of experimental procedures. Several graphic items in this figure have been generated  
 121 with the help of Adobe® Firefly™ Artificial Intelligence generator.

Formatted: Superscript  
 Formatted: Superscript  
 Formatted: Font: Not Bold

122 2.1. Effects of storage time and inhibitors on the quantification of dissolved gases

123 *Study site and sampling*

CO<sub>2</sub> overestimation from HgCl<sub>2</sub> fixation – Clayer et al.

124 Surface water was collected from Lake Svartkulp (59.9761313 N, 10.7363544 E; Southeast Norway)  
125 north of Oslo, Norway, on the 4<sup>th</sup> of September 2019. A 5 L plastic bottle was gently pushed into the  
126 water and progressively tilted to let the water flow into the bottles without bubbling. The bottle  
127 aperture was covered with a 90 µm plankton net to avoid sampling large particles. This procedure was  
128 repeated five times to yield a total water volume of 25 L. The 5 L water bottles were immediately  
129 brought back to the lab. Upon arrival at the laboratory, after temperature equilibration, water from the  
130 5 L bottles was slowly poured, to limit gas exchange with the ambient air, into a 25 L tank to provide  
131 a single bulk sample to start the incubation experiment. Filtration, e.g., with 0.45 or 0.2 µm filters,  
132 was avoided to minimize changes in dissolved gas concentrations (e.g., Magen et al., 2014). The  
133 mixed water sample (25 L) was sub-sampled (0.5 L) for the determination of alkalinity (127 µmol L<sup>-1</sup>,  
134 pH (6.73), ammonium (3 µg N L<sup>-1</sup>), nitrate (5 µg N L<sup>-1</sup>), total N (230 µg N L<sup>-1</sup>), phosphate (1 µg P  
135 L<sup>-1</sup>), total P (9 µg P L<sup>-1</sup>) and TOC (8.9 mg C L<sup>-1</sup>) all analysed by standard methods at the accredited  
136 Norwegian Institute for Water Research (NIVA) lab (see Tab. S1). *In situ* temperature of the lake  
137 water was measured with a handheld thermometer and was 18.5 °C. Note that particulate organic  
138 carbon is a negligible fraction of TOC in Norwegian lake waters, representing on average less than  
139 3% (de Wit et al., 2023).

140 Lake Svartkulp was selected for this experiment because it is representative of low ionic strength  
141 Northern Hemisphere lakes, typically found in granitic bedrock regions in North-East America and  
142 Scandinavia. It is a typical low-productivity, heterotrophic, slightly acidic to neutral, moderately  
143 humic lake. Similar lakes are found in Southern Norway (de Wit et al., 2023), large parts of Sweden  
144 (Valina et al. 2014), Finland, Atlantic Canada (Houle et al., 2022), Ontario, Québec, and North-East  
145 USA (Skjelkvåle and de Wit 2011; Weyhenmeyer et al., 2019).

#### 146 *Laboratory incubation experiment with different preservatives and storage times*

147 The experimental design involved to incubate 72 borosilicate glass bottles (120 mL) filled with lake  
148 water from our 25 L bulk sample ~~subjected and submitted~~ to four different treatments: addition of  
149 240 µL of a preservative solution of (i) HgCl<sub>2</sub>, (ii) CuCl<sub>2</sub> or a (iii) AgNO<sub>3</sub>, or addition of 240 µL of  
150 (iv) MilliQ water. The bottles amended with MilliQ water are hereafter referred to as “unfixed”. The  
151 72 bottles were divided into three groups which were incubated cold (+4°C) and dark for 24h, three  
152 weeks or three months respectively, before being processed for dissolved gas analysis by gas  
153 chromatography. These incubation times were selected to represent situations where samples are  
154 processed directly upon return to the laboratory (24h), or after medium (3 weeks) to long (3 months) -  
155 term storage, respectively. At each time point and for each treatment, a group of 6 bottles were further  
156 processed for dissolved gas analysis. Concentrations of O<sub>2</sub>, N<sub>2</sub>, N<sub>2</sub>O, CO<sub>2</sub> and CH<sub>4</sub> were determined  
157 by gas chromatography (see below) using the headspace technique following Yang *et al.* (2015). pH  
158 was not measured at the end of the storage period.

CO<sub>2</sub> overestimation from HgCl<sub>2</sub> fixation – Clayer et al.

159 In details, within 3h of lake water sampling, the 120mL bottles were gently filled with water from the  
160 mixed sample (25 L). Each 120mL bottle was slowly lowered into the water and progressively tilted  
161 to let the water flow into the bottle without bubbling. The bottle was then capped under water with a  
162 gas tight butyl rubber stopper after ensuring that there were no air bubbles in the bottle. The bottles  
163 were randomized prior to preservative or MilliQ ~~amendment~~~~treatment~~. The preservative ~~solution~~-or  
164 MilliQ amendment was pushed in each bottle with a syringe and needle through the rubber septum.  
165 To avoid overpressure, another needle was placed through septum at the same time, at least 2 cm  
166 above the other needle, to allow an equivalent volume of clean water to be released.

167 Stock solutions of HgCl<sub>2</sub>, CuCl<sub>2</sub> and AgNO<sub>3</sub> were prepared according to Tab. 1 using high accuracy  
168 chemical equipment (e.g., high accuracy scale, volumetric flasks). The Ag (Silver nitrate EMSURE®  
169 ACS; Merck KGaA, Germany) Cu (Copper(II) chloride dihydrate; Merck Life Science ApS, Norway)  
170 and Hg (Mercury(II) chloride; undetermined) salts were dissolved in MilliQ ultrapure water (>18 MΩ  
171 cm). For measurement of CO<sub>2</sub> in seawater samples, the standard method involves poisoning the  
172 samples by adding a saturated HgCl<sub>2</sub> solution in a volume equal to 0.05-0.02% of the total volume  
173 (Dickson 2007). We used this as a starting point and added 0.02 % saturated HgCl<sub>2</sub> solution to 18  
174 bottles (240 μL of HgCl<sub>2</sub> 10× diluted saturated solution), resulting in a sample concentration of 14 μg  
175 HgCl<sub>2</sub> mL<sup>-1</sup> (51.6 μM; Tab. 1). Based on estimated toxicity relative to Hg (Deheyn et al., 2004; Halmi  
176 et al., 2019), the silver and copper salts were added in molar concentrations equal to two and three  
177 times the molar concentration of HgCl<sub>2</sub>, respectively (Tab. 1), although it varies between species of  
178 microorganisms and environmental matrices (Hassen *et al.*, 1998; Rai, Gaur & Kumar, 1981).

179 **Table 1.** Stock and sample concentrations of HgCl<sub>2</sub>, CuCl<sub>2</sub> and AgNO<sub>3</sub>.

Salt	Stock solution	Sample concentration	Rationale
HgCl <sub>2</sub>	70 g/L (saturated)	14.0±0.01 μg/mL (51.6 μM)	Dickson, Sabine & Christian, 2007
CuCl <sub>2</sub>	131.9 g/L	26.4±0.02 μg/mL (154.7 μM)	3 × Hg
AgNO <sub>3</sub>	87.6 g/L	17.5±0.02 μg/mL (103.1 μM)	2 × Hg

Formatted Table

180

181 *Additional 24h incubation experiment with different preservatives for pH measurements*

182 Since pH was not measured at the end of the first incubation experiment, we performed an additional  
183 experiment to document any potential rapid (within 24h) impacts of preservative on pH. A total of 48  
184 borosilicate glass bottles (120 mL) filled with lake water were ~~submitted~~~~subjected~~ to the same four  
185 different treatments as the first experiment described above: HgCl<sub>2</sub>, CuCl<sub>2</sub>, AgNO<sub>3</sub> or MilliQ water  
186 amendments. To this end, a 20L water tank was filled with surface water from Lake Svartkulp on the  
187 14<sup>th</sup> of December 2023. The water tank was immediately returned to the laboratory and left for 24h to  
188 equilibrate to the room temperature. On December 15<sup>th</sup>, 120mL bottles were gently filled with water

CO<sub>2</sub> overestimation from HgCl<sub>2</sub> fixation – Clayer et al.

189 from the bulk 20L sample, as described above. The bottles were randomized prior to preservative or  
190 MilliQ ~~amendment-treatment~~ performed as described above. The bottles were then incubated at room  
191 temperature for 2h or 24h. pH was measured in the initial unamended lake water, in 24 bottles opened  
192 after 2h incubation, and in 24 bottles opened after 24h incubation. pH measurements were performed  
193 with a WTW Multi 3620 pH meter calibrated using a two-point calibration at pH = 4 and pH = 7. All  
194 pH measures were corrected for temperature. Water temperature of the water samples during pH  
195 measurements ranged between 19.1 and 21.2°C.

196

197 2.2. Effects of HgCl<sub>2</sub> on dissolved CO<sub>2</sub> analyses over a range of pH values

198 *Study site and sampling*

199 Water samples were collected from Lake Lundebyvannet located southeast of Oslo (59.54911 N,  
200 11.47843 E, Southeast Norway). Two sets of samples were taken from 1, 1.5, 2 and 2.5 m depth  
201 using a water sampler once or twice a week between April 2020 and January 2021 for the  
202 determination of (i) dissolved CO<sub>2</sub> by GC analysis following fixation with HgCl<sub>2</sub> and (ii) DIC  
203 analysis with a TOC analyser. Samples for GC analysis were filled into 120 mL glass bottles (as  
204 described above for the 72 incubation bottles), which were sealed with rubber septa under water  
205 without air bubbles. Samples for GC analysis were preserved in the field by adding a half-saturated (at  
206 20°C) solution of HgCl<sub>2</sub> (150 µL) through the rubber seal of each bottle using a syringe, as described  
207 above the 72 incubation bottles, resulting in a concentration of 161 µM similar to previous studies  
208 (Clayer et al., 2021; Hessen et al., 2017; Yang et al., 2015). Samples for DIC analysis were filled  
209 without bubbles in 100 ml Winkler glass bottles that were sealed airtight directly after sampling.  
210 These samples were not fixed in any way and were analysed by a TOC analyzer within two hours.

211 Note that estimation of dissolved CO<sub>2</sub> concentrations from pH and DIC is the least uncertain method  
212 of indirect CO<sub>2</sub> concentration with estimated relative error of 6% or less (Golub et al., 2017). Lake  
213 water temperature and pH were measured *in-situ* using HOBO pH data loggers placed at 1, 1.5, 2 and  
214 2.5 m (Elit, Gjerdrum, Norway).

Formatted: Subscript

Formatted: Subscript

215 Lake Lundebyvannet has a surface area of 0.4 km<sup>2</sup> and a maximum depth of 5.5 m. It often  
216 experiences large blooms of *G. semen* over the summer between May and September (Hagman et al.,  
217 2015; Rohrlack, 2020). The lake water is characterised by high and fluctuating concentrations of  
218 humic substances (with DOC concentrations ranging from 8 to 28 mg C L<sup>-1</sup>), ammonium (5 to 100 µg  
219 N L<sup>-1</sup>), nitrate (20 to 700 µg N L<sup>-1</sup>), total N (average of 612 µg N L<sup>-1</sup>), phosphate (2 to 4 µg P L<sup>-1</sup>),  
220 total P (average of 28 µg P L<sup>-1</sup>; Rohrlack et al., 2020; Hagman et al., 2015), a fluctuating pH (from 5.5  
221 to 7.3), weak ionic strength with alkalinity ranging between 30 and 150 µmol L<sup>-1</sup>, and electric  
222 conductivity varying from 40 to 70 µS cm<sup>-1</sup>. For more details, see Rohrlack *et al.* (2020).



CO<sub>2</sub> overestimation from HgCl<sub>2</sub> fixation – Clayer et al.

223 Lake Lundebyvannet was selected for this experiment because it is representative of productive, low-  
224 ionic strength Northern Hemisphere lakes typically found in the southern part of granitic bedrock  
225 regions in North-East America and Scandinavia.

### 226 2.3. Analytical chemistry

#### 227 *Gas chromatography*

228 Headspace was prepared by gently backfilling sample bottles with 20–30 mL helium (He; 99,9999%)  
229 into the closed bottle while removing a corresponding volume of water. Care was taken to control the  
230 headspace pressure within 5% of ambient and a slight He overpressure was released before  
231 equilibration. The bottles were shaken horizontally at 150 rpm for 1 h to equilibrate gases between  
232 sample and headspace. The temperature during shaking was recorded by a data logger. Immediately  
233 after shaking, the bottles were placed in an autosampler (GC-Pal, CTC, Switzerland) coupled to a gas  
234 chromatograph (GC) with He back-flushing (Model 7890A, Agilent, Santa Clara, CA, US).  
235 Headspace gas was sampled (approx. 2 mL) by a hypodermic needle connected to a peristaltic pump  
236 (Gilson Minipuls 3), which connected the autosampler with the 250 µL heated sampling loop of the  
237 GC.

238 The GC was equipped with a 20-m wide-bore (0.53 mm) Poraplot Q column for separation of CH<sub>4</sub>,  
239 CO<sub>2</sub> and N<sub>2</sub>O and a 60 m wide-bore Molsieve 5Å PLOT column for separation of O<sub>2</sub> and N<sub>2</sub>, both  
240 operated at 38°C and with He as carrier gas. N<sub>2</sub>O and CH<sub>4</sub> were measured with an electron capture  
241 detector run at 375°C with Ar/CH<sub>4</sub> (80/20) as makeup gas, and a flame ionization detector,  
242 respectively. CO<sub>2</sub>, O<sub>2</sub>, and N<sub>2</sub> were measured with a thermal conductivity detector (TCD). Certified  
243 standards of CO<sub>2</sub>, N<sub>2</sub>O, and CH<sub>4</sub> in He were used for calibration (AGA, Germany), whereas air was  
244 used for calibrating O<sub>2</sub> and N<sub>2</sub>. The analytical error for all gases was lower than 2%. For the Lake  
245 Lundebyvannet time series, CO<sub>2</sub> was separated from other gases using the 20 m wide-bore (0.53 mm)  
246 Poraplot Q column while the other gases were not measured.

247 The results from gas chromatography give the relative concentration of dissolved gases (in ppm) in  
248 the headspace in equilibrium with the water. For the lab experiment with Svartkulp samples (section  
249 2.1), the concentration of dissolved gases in the water at equilibrium with the headspace were  
250 calculated from the temperature corrected Henry constant in water using Carroll, Slupsky and Mather  
251 (1991) for CO<sub>2</sub>, Weiss and Price (1980) for N<sub>2</sub>O, Yamamoto, Alcauskas and Crozier (1976) for CH<sub>4</sub>,  
252 Millero, Huang and Laferiere (2002) for O<sub>2</sub>, Hamme and Emerson (2004) for N<sub>2</sub>. For the Lake  
253 Lundebyvannet time series (section 2.2), the concentration of CO<sub>2</sub> in the water samples were  
254 determined using temperature-dependent Henry's law constants given by Wilhelm, Battino and  
255 Wilcock (1977). The quantities of gases in the headspace and water were summed to find the  
256 concentrations and partial pressures of dissolved gases from the water collected in the field as follows:

CO<sub>2</sub> overestimation from HgCl<sub>2</sub> fixation – Clayer et al.

$$[gas] = \frac{p_{gas}HV_{water} + \frac{p_{gas}V_{headspace}}{RT}}{V_{water}} \quad (\text{Eq. 1})$$

where [gas] is the gas aqueous concentration,  $p_{gas}$  is the gas partial pressure,  $H$  is the Henry constant,  $V_{water}$  is the volume of water sample during headspace equilibration,  $V_{headspace}$  is the headspace gas volume during equilibration,  $R$  is the gas constant and  $T$  the temperature during headspace equilibration (recorded during shaking). The calculations were similar to Yang *et al.* (2015).

262

### 263 DIC analyses

264 DIC analysis was performed for the Lake Lundebyvannet time series using a Shimadzu TOC-V CPN  
265 (Oslo, Norway) instrument equipped with a non-dispersive infrared (NDIR) detector with O<sub>2</sub> as a  
266 carrier gas at a flow rate of 100 mL min<sup>-1</sup>. Two to three replicate measurements were run per sample.  
267 The system was calibrated using a freshly prepared solution containing different concentrations of  
268 NaHCO<sub>3</sub> and Na<sub>2</sub>CO<sub>3</sub> and standards were measured in between each 6<sup>th</sup> sample. CO<sub>2</sub> concentrations  
269 in water samples ([CO<sub>2</sub>]) were calculated on the bases of temperature, pH and DIC concentrations as  
270 follows (Rohrlack *et al.*, 2020):

$$[CO_2] = \frac{[H^+]^2 C_T}{Z} \quad (\text{Eq. 2})$$

272 where  $[H^+]$  is the proton concentration ( $10^{-pH}$ ),  $C_T$  is the dissolved inorganic carbon concentration  
273 and  $Z$  is given by:

$$Z = [H^+]^2 + K_1[H^+] + K_1K_2 \quad (\text{Eq. 3})$$

275 where  $K_1$  and  $K_2$  are the first and second carbonic acid dissociation constant adjusted for temperature  
276 ( $pK_1 = 6.41$  and  $pK_2 = 10.33$  at 25°C; Stumm & Morgan, 1996).

277

### 278 2.4. Data analysis

#### 279 *pCO<sub>2</sub> and saturation deficit*

280 Lake Lundebyvannet CO<sub>2</sub> concentrations provided by GC and DIC analyses were converted to pCO<sub>2</sub>  
281 (in µatm) as follows:

$$pCO_2 = \frac{[CO_2]}{0.987 \times K_H P_{atm}} \quad (\text{Eq. 4})$$

283 where  $K_H$  is Henry constant for CO<sub>2</sub> adjusted for in-situ water temperature (Stumm & Morgan, 1996)  
284 and  $P_{atm}$  is the atmospheric pressure in bar approximated by:

Formatted: Superscript

CO<sub>2</sub> overestimation from HgCl<sub>2</sub> fixation – Clayer et al.

285 
$$P_{atm} = (1013 - 0.1 \times altitude) \times 0.001 \quad (\text{Eq. 5})$$

286 where *altitude* is the altitude above sea level of Lake Lundebyvannet (158 m). Finally, the CO<sub>2</sub>  
287 saturation deficit ( $Sat_{CO_2}$  in  $\mu\text{atm}$ ) was given by

288 
$$Sat_{CO_2} = pCO_2 - [CO_2]_{air} \quad (\text{Eq. 6})$$

289 where  $[CO_2]_{air}$  is the pCO<sub>2</sub> in the air (416  $\mu\text{atm}$  for 2020 in Southern Norway retrieved from EBAS  
290 database; NILU, 2022; Tørseth et al., 2012).  $Sat_{CO_2}$  gives the direction of CO<sub>2</sub> flux at the water-  
291 atmosphere interface, and its product with gas transfer velocity determine the CO<sub>2</sub> flux at the water-  
292 atmosphere interface, i.e., whether lake ecosystems are sink ( $Sat_{CO_2} < 0$ ) or source ( $Sat_{CO_2} > 0$ ) of  
293 atmospheric CO<sub>2</sub>.

294

#### 295 *Statistical analyses*

296 The effect of storage time and treatment on five dissolved gases (O<sub>2</sub>, N<sub>2</sub>, CO<sub>2</sub>, CH<sub>4</sub>, N<sub>2</sub>O) from the  
297 Lake Svartkulp samples was tested with a two-way ANOVA at an alpha level adapted using the  
298 Bonferroni correction for multiple testing, i.e.,  $\alpha=0.05/5=0.01$ . To evaluate the impact of Hg fixation  
299 on Lake Lundebyvannet samples,  $[CO_2]$  values determined by headspace equilibration and GC  
300 analysis of HgCl<sub>2</sub>-fixed samples were compared with those calculated from DIC measurements of  
301 unfixed samples with a paired t-test.

302 A regression analysis was performed to describe the overestimation of CO<sub>2</sub> concentrations caused by  
303 HgCl<sub>2</sub> fixation in Lake Lundebyvannet samples as a function of pH. The total CO<sub>2</sub> concentration in  
304 the HgCl<sub>2</sub>-fixed samples ( $[CO_2]_{HgCl_2}$ ) can be expressed as:

305 
$$[CO_2]_{HgCl_2} = [CO_2]_i + [CO_2]_{ex} \quad (\text{Eq. 7})$$

306 where  $[CO_2]_i$  is the initial CO<sub>2</sub> concentration prior to HgCl<sub>2</sub> fixation, i.e., CO<sub>2</sub> concentration in the  
307 unfixed samples, and  $[CO_2]_{ex}$  is the excess CO<sub>2</sub> concentration caused by a decrease in pH following  
308 HgCl<sub>2</sub> fixation. The relative CO<sub>2</sub> overestimation ( $E$  in %) is given by:

309 
$$E = \frac{[CO_2]_{HgCl_2} - [CO_2]_i}{[CO_2]_i} = \frac{[CO_2]_{ex}}{[CO_2]_i} \quad (\text{Eq. 8})$$

310 The impact of pH (or  $[H^+]$ ) on  $E$  was mathematically described by running a regression analysis  
311 using MATLAB®. The *fminsearch* MATLAB function from the Optimization toolbox was used to  
312 find the minimum sum of squared residuals (SSR) for functions of the form of:  $E = A/[H^+]$  or  $E =$   
313  $A \times 10^{-B \times pH}$ . For each optimal solution, the root-mean-square error (RMSE) and coefficient of  
314 determination ( $R^2$ ) were calculated against observed values of  $E$ , i.e., values of  $E$  determined  
315 empirically from observed  $[CO_2]_i$  and  $[CO_2]_{ex}$ .

CO<sub>2</sub> overestimation from HgCl<sub>2</sub> fixation – Clayer et al.

316

317 *Chemical speciation, saturation-index calculations, and prediction of CO<sub>2</sub> overestimation*

318 The speciation of solutes and saturation index values (SI) of selected minerals were calculated with  
319 the program PHREEQC developed by the USGS (Parkhurst & Appelo, 2013), neglecting the effect of  
320 dissolved organic matter. This was used to assess the impact of the addition of preservative on pH and  
321 shifting the carbonate equilibrium as well as dissolved inorganic carbon losses due to carbonate  
322 mineral precipitation. PHREEQC is commonly used to calculate the speciation of inorganic carbon,  
323 the SI of carbonate minerals and to help estimate the fate of inorganic carbon in carbon cycling  
324 studies (Atekwana et al. 2016; Clayer et al. 2016; Klaus 2023). For each PHREEQC simulation, two  
325 files, respectively the database (with input reactions) and input files, were used to define the  
326 thermodynamic model and the type of calculations to perform. The database of MINTQA2 (e.g.,  
327 *minteq.dat*, Allison et al., 1991) was used to describe the chemical system because it includes, inter  
328 alia, reactions and constants for Ag, Cu and Hg complexation with Cl, NO<sub>3</sub> and carbonates. ~~In total,~~  
329 Three PHREEQC simulations were run representing the addition of each preservative solution to  
330 sample water from Lake Svartkulp. The input files described the composition of two aqueous  
331 solutions: (i) the preservative solution assumed to contain only the preservative (i.e., HgCl<sub>2</sub> solution)  
332 and (ii) sample water from Lake Svartkulp with observed major element concentrations (pH, Al, Ca,  
333 Cl, Cu, Fe, Mg, Mn, N as nitrate, K, Na, S as sulfate, Zn; Tab. S1) and Hg and Ag natural  
334 concentration assumed to be 10<sup>-5</sup> mg/L. The output file provided the activities of the various solutes in  
335 the preserved samples, i.e., simulating the mixing of 120 mL of lake water with 240 µL of the AgNO<sub>3</sub>,  
336 CuCl<sub>2</sub> and HgCl<sub>2</sub> preservative solutions, as described in section 2.1. This procedure allows to estimate  
337 the pH of the preserved samples as well as SI for various mineral phases. The SI is calculated by  
338 PHREEQC comparing the chemical activities of the dissolved ions of a mineral (ion activity product,  
339 IAP) with their solubility product (K<sub>s</sub>). When SI > 1, precipitation is thermodynamically favourable.  
340 Note However, that PHREEQC does not give information about precipitation kinetics.

341 Similarly, PHREEQC was ~~also~~ used to estimate the decrease in pH caused by adding 150 µL of a  
342 half-saturated HgCl<sub>2</sub> solution to Lake Lundebyvannet samples prior to GC analyses, as described in  
343 section 2.2. In absence of data on the chemical composition of Lake Lundebyvannet, we assumed that  
344 it had the same composition as Lake Svartkulp water samples. This assumption is supported by the  
345 fact that waters from both lakes have circumneutral pH, low ionic strength (poor buffering capacity)  
346 and high DOC concentration and would therefore behave similarly in presence of acids. Briefly, for  
347 each 0.1 pH value between pH of 5.4 and 7.3, the carbonate alkalinity was first adjusted by increasing  
348 HCO<sub>3</sub> concentrations in the input files for PHREEQC to confirm that the water was at equilibrium at  
349 the given pH value. Then, the effect of adding 150µL of a half-saturated HgCl<sub>2</sub> solution was  
350 simulated as described above for Lake Svartkulp. Knowing the new equilibrated pH, after addition of

Formatted: Subscript

CO<sub>2</sub> overestimation from HgCl<sub>2</sub> fixation – Clayer et al.

351 HgCl<sub>2</sub>, the overestimation of CO<sub>2</sub> concentration in Hg-fixed samples relative to unfixed samples (*E*,  
352 described in Eq. 8 above) can be predicted as described below.

353 Adapting Eq. (2), we obtain:

$$354 \quad [CO_2]_{HgCl_2} = \frac{[H^+]_{HgCl_2}^2 C_T}{Z_{HgCl_2}} \quad (\text{Eq. 9})$$

355 and

$$356 \quad [CO_2]_i = \frac{[H^+]_i^2 C_T}{Z_i} \quad (\text{Eq. 10})$$

357 where  $[H^+]_i$  is the proton concentration measured in the initial water samples prior to HgCl<sub>2</sub> fixation,  
358 and  $[H^+]_{HgCl_2}$  is the proton concentration estimated by PHREEQC following HgCl<sub>2</sub> fixation, and  
359 similarly for  $Z_i$  and  $Z_{HgCl_2}$  from Eq. (3). Combining Eqs. (7), (9) and (10) we obtain:

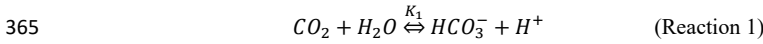
$$360 \quad [CO_2]_{ex} = C_T \left( \frac{[H^+]_{HgCl_2}^2}{Z_{HgCl_2}} - \frac{[H^+]_i^2}{Z_i} \right) \quad (\text{Eq. 11})$$

361 Hence:

$$362 \quad E = \frac{[CO_2]_{ex}}{[CO_2]_i} = \frac{\left( \frac{[H^+]_{HgCl_2}^2}{Z_{HgCl_2}} - \frac{[H^+]_i^2}{Z_i} \right)}{\frac{[H^+]_i^2}{Z_i}} \quad (\text{Eq. 12})$$

363

364 Alternatively, *E* can also simply be predicted based on the carbonic acid dissociation:



366 At equilibrium, we have:

$$367 \quad K_1 = \frac{[HCO_3^-][H^+]}{[CO_2]} \quad (\text{Eq. 13})$$

368 When pH is decreased upon addition of HgCl<sub>2</sub>, a fraction ( $\alpha$ ) of the initial bicarbonate concentration  
369  $[HCO_3^-]_i$  is turned into CO<sub>2</sub>. This fraction, expressed as  $[CO_2]_{ex}$  in Eq. (7) above, can be estimated  
370 with Eq. 13 as follows:

$$371 \quad [CO_2]_{ex} = \alpha [HCO_3^-]_i = \frac{\alpha K_1 [CO_2]_i}{[H^+]_i} \quad (\text{Eq. 14})$$

372 Introducing the expression of  $[CO_2]_{ex}$  from Eq. 14 into Eq. 8 yields:

$$373 \quad \frac{[CO_2]_{ex}}{[CO_2]_i} = E = \frac{\alpha K_1}{[H^+]_i} \quad (\text{Eq. 15})$$

CO<sub>2</sub> overestimation from HgCl<sub>2</sub> fixation – Clayer et al.

374 When the decrease in pH, or acidification, is greater than the buffering capacity of the water:  $\alpha = 1$ .  
375 The value of  $\alpha$  cannot exceed 1 because the amount of CO<sub>2</sub> produced by a decrease in pH cannot  
376 exceed the amount of HCO<sub>3</sub><sup>-</sup> initially present. In all the other cases, we have:  $\alpha < 1$ . For both  
377 predictions of  $E$ , i.e., with Eqs. 12 and 15, the root-mean-square error (RMSE) and coefficient of  
378 determination (R<sup>2</sup>) were calculated.

379 Finally, additional sources of CO<sub>2</sub> overestimation were investigated by analysing the residuals of the  
380 model described by Eq. 12, i.e., the difference between  $E$  predicted with Eq. 12 and  $E$  determined  
381 empirically with Eq. 8. Briefly, residuals were plotted against pH and *in situ* temperature. Residuals  
382 were separated in two groups based on the empirical value of  $[HCO_3^-]_i - [CO_2]_{ex}$ , i.e., the first group  
383 had values of  $[HCO_3^-]_i - [CO_2]_{ex} \geq a$  while the second group had values of  $[HCO_3^-]_i - [CO_2]_{ex} \leq$   
384  $-a$  where different values for  $a$  were used: 20, 10 or 5  $\mu$ M. The justification for separating residuals  
385 in two groups is that: (i) the first group represents samples for which bicarbonate alkalinity in the  
386 original sample is, as expected, higher than CO<sub>2</sub> overestimation after HgCl<sub>2</sub>-fixation, while (ii) the  
387 second group represents samples for which bicarbonate alkalinity is not sufficient to explain CO<sub>2</sub>  
388 overestimation after HgCl<sub>2</sub>-fixation.

389

390 *CO<sub>2</sub> diffusion fluxes from Lake Lundebyvannet*

391 The diffusive flux of CO<sub>2</sub> ( $F_{CO_2}$  in mol m<sup>-2</sup> d<sup>-1</sup>) from Lake Lundebyvannet surface water was  
392 estimated according to:

393 
$$F_{CO_2} = \frac{k_{CO_2}([CO_2] - [CO_2]_{eq})}{1000} \quad (\text{Eq. 16})$$

394 where  $k_{CO_2}$  is the CO<sub>2</sub> transfer velocity in m d<sup>-1</sup>,  $[CO_2]$  is the surface water CO<sub>2</sub> concentration ( $\mu$ M),  
395 and 1000 is a factor to ensure consistency in the units and  $[CO_2]_{eq}$  is the theoretical water CO<sub>2</sub>  
396 concentration ( $\mu$ M) in equilibrium with atmospheric CO<sub>2</sub> concentration calculated with Eq. (3) and  
397 pCO<sub>2</sub> of 416  $\mu$ atm (see above).

398 The CO<sub>2</sub> transfer velocity ( $k_{CO_2}$ ) was estimated as follows (Vachon & Prairie, 2013):

399 
$$k_{CO_2} = k_{600} \left( \frac{600}{Sc_{CO_2}} \right)^{-n} \quad (\text{Eq. 17})$$

400 where  $k_{600}$  is the gas transfer velocity (m d<sup>-1</sup>) estimated from empirical wind-based models and  $Sc_{CO_2}$   
401 is the CO<sub>2</sub> Schmidt number for in situ water temperature (unitless; Wanninkhof, 2014). We used  $n$   
402 values of 0.5 or 2/3 when wind speed was below or above 3.7 m s<sup>-1</sup>, respectively (Gu erin et al., 2007).  
403 Empirical  $k_{600}$  models included those from Cole & Caraco (1998;  $k_{600} = 2.07 + 0.215U_{10}^{1.7}$ ),  
404 Vachon & Prairie (2013;  $k_{600} = 2.51 + 1.48U_{10} + 0.39U_{10} \log_{10} LA$ ) and Crusius & Wanninkhof

CO<sub>2</sub> overestimation from HgCl<sub>2</sub> fixation – Clayer et al.

405 (2003; power model:  $k_{600} = 0.228U_{10}^{2.2} + 0.168$  in cm h<sup>-1</sup>).  $U_{10}$  and  $LA$  refer to mean wind speed at  
406 10 m in m s<sup>-1</sup> and lake area in km<sup>2</sup>, respectively. Sub-hourly  $U_{10}$  data for 2020 was retrieved from a  
407 weather station of the Norwegian Meteorological Institute located 1.5 km west of Lake  
408 Lundebyvannet (station name: E18 Melleby; ID: SN 3480; 59.546 N, 11.4535E) using the Frost  
409 application programming interface (*Frost API*, 2022). Daily, monthly, and yearly (only covering the  
410 ice-free season: April–November)  $F_{CO_2}$  was estimated using Eq. (12). Daily [CO<sub>2</sub>] was interpolated  
411 from weekly data using a modified Akima spline (makima spline in Matlab® based on Akima, 1974).  
412 This interpolation method is known to avoid excessive local undulations.

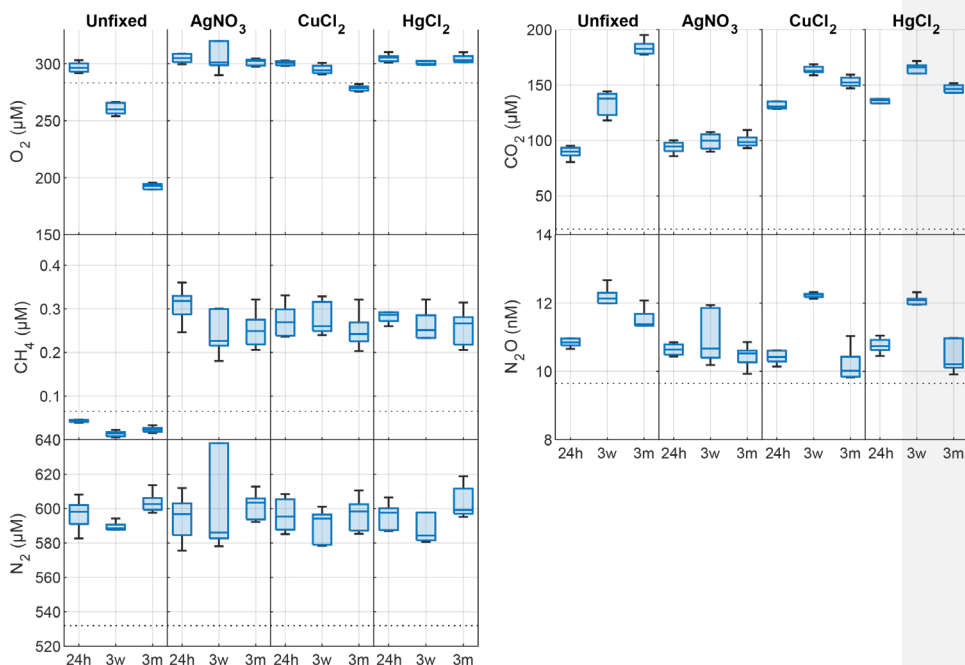
### 413 3. Results

#### 414 3.1. Effects of preservatives and storage time on dissolved gases

415 In the unfixed samples from Lake Svartkulp, the concentration of O<sub>2</sub> declined while CO<sub>2</sub> increased  
416 over time in a close to 1:1 molar ratio, likely reflecting the effect of microbial respiration activity and  
417 mineralisation of organic matter (Fig. +2, Tab. S2). Concentration of O<sub>2</sub> in the unfixed samples  
418 decreased from near 300 to below 200 μM (Fig. +2). In the presence of inhibitors, O<sub>2</sub> concentrations  
419 tended to be slightly higher at t=24h and remained constant or declined only slightly over time to  
420 generally remain at or above saturation (280 to 300 μM). Thus, the inhibitors were effective in  
421 reducing oxic respiration.

422 The concentration of CO<sub>2</sub> in the presence of AgNO<sub>3</sub> at t = 24h was not significantly different to the  
423 unfixed at t = 0 (Fig +2; paired t-test,  $P > 0.1$ ). At t = 24h, CO<sub>2</sub> concentrations were however much  
424 higher in the presence of HgCl<sub>2</sub> (135 μM) or CuCl<sub>2</sub> (131 μM) than in the unfixed (89 μM; Fig +2,  
425 Tab. S2). The CO<sub>2</sub> further increases from 130 μM to ~160 μM after 3 weeks in both sample sets  
426 preserved with HgCl<sub>2</sub> and CuCl<sub>2</sub> while a decrease in O<sub>2</sub> is less pronounced for samples fixed with  
427 CuCl<sub>2</sub> and completely absent for samples fixed with HgCl<sub>2</sub>. Overall, the addition of HgCl<sub>2</sub> or CuCl<sub>2</sub>  
428 following sampling increased CO<sub>2</sub> concentrations by 47% after 24h compared to the unfixed and  
429 caused further changes over the three-month storage time, while preservation with AgNO<sub>3</sub> yielded  
430 CO<sub>2</sub> concentrations consistent with the unfixed and caused negligible changes over time (Fig. +2;  
431 paired t-test,  $P > 0.1$ ).

432 The concentration of CH<sub>4</sub> across all samples ranged between 0.017 and 0.377 μM (Fig. +2), as  
433 expected two orders of magnitude smaller than CO<sub>2</sub>. At t = 24h, the concentration of CH<sub>4</sub> was over  
434 0.2 μM in the presence of inhibitors while it was below saturation in the unfixed (0.03 μM; Fig. +2).  
435 CH<sub>4</sub> oversaturation in the preserved samples persisted after three weeks and three months of storage  
436 and CH<sub>4</sub> concentration remained unchanged (Fig. +2, Tab. S2).



437

438 **Fig 12.** Changes in dissolved O<sub>2</sub>, CO<sub>2</sub>, CH<sub>4</sub>, N<sub>2</sub>O and N<sub>2</sub> concentrations (nM or µM) in the absence  
 439 (unfixed) and presence of different preservatives (AgNO<sub>3</sub>, CuCl<sub>2</sub>, HgCl<sub>2</sub>) at three times (24h, 24h  
 440 after incubation start; 3w, three weeks after collection; 3m, three months after collection). The  
 441 horizontal dotted line is the saturated gas concentration corresponding to 100% gas saturation at *in*  
 442 *situ* lake temperature. Box plots show the median, 25<sup>th</sup> and 75<sup>th</sup> percentiles and the whiskers display  
 443 ~~all data coverage~~ minimum and maximum.



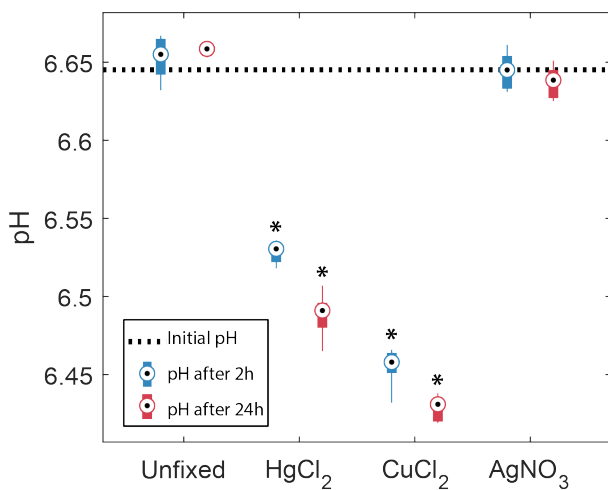
444 The concentration of N<sub>2</sub>O ranged between 9.8 and 12.7 nM with only samples preserved with AgNO<sub>3</sub>  
445 showing negligible changes over time (Fig. 42; paired t-test, P>0.1). All the other samples showed  
446 consistent patterns with storage time. N<sub>2</sub>O concentrations initially increased within the first 3 weeks,  
447 followed by a decrease after 3 months.

448 The changes in N<sub>2</sub> were likely within handling and analytical errors and not different in the presence  
449 or absence of inhibitors (Fig. 42; Tab. S2; paired t-test, P>0.1).

450

### 451 3.2. Effects of preservatives on pH

452 In the samples amended with ultrapure water or AgNO<sub>3</sub>, the pH did not show any significant changes  
453 after 2h or 24h. In contrast, both groups with HgCl<sub>2</sub> and CuCl<sub>2</sub> amendments-treatments show  
454 significant decreases of pH after 2h, -0.12 and -0.19, respectively, and 24h, -0.16 and -0.21,  
455 respectively. In addition, they showed a significant decrease in pH from 2h to 24h. Samples amended  
456 with CuCl<sub>2</sub> show the strongest decrease in pH.



457

458 **Fig 23.** Observed changes in pH in the absence (unfixed) and presence of different preservatives  
459 (AgNO<sub>3</sub>, CuCl<sub>2</sub>, HgCl<sub>2</sub>) at two times, 2h and 24h after the start of the incubation. The horizontal  
460 dotted line represents the initial pH of the bulk water sample. Box plots show the median, 25<sup>th</sup> and  
461 75<sup>th</sup> percentiles and the whiskers display all data coverage minimum and maximum of the 6 replicates.  
462 Stars indicate groups that are significantly different from each other and from the initial pH (two-way  
463 ANOVA).

464 3.3. Contrasting impacts of HgCl<sub>2</sub>, CuCl<sub>2</sub> and AgNO<sub>3</sub> on dissolved CO<sub>2</sub> estimation revealed by  
465 chemical speciation modelling

CO<sub>2</sub> overestimation from HgCl<sub>2</sub> fixation – Clayer et al.

466 The PHREEQC simulation of unpreserved samples, based on concentrations of all major elements  
467 (Tab. S1), predicted a pH of 6.72 (Tab. 2) which is very close to the measured pH of 6.73 (Tab. S1).  
468 This suggests that chemical information provided to PHREEQC is likely sufficient to describe the  
469 system, without having to invoke more complex reactions with dissolved organic matter. The addition  
470 of HgCl<sub>2</sub> and CuCl<sub>2</sub> both caused a significant decrease in pH to 6.40 and 6.45, respectively (Tab. 2)  
471 which is similar to the decrease observed at the end of the 24h short term incubation (Fig. 2).

472 In absence of preservatives, none of the common carbonate minerals, including calcite, were  
473 associated with a saturation index higher than 1, i.e., dissolution was thermodynamically favourable  
474 for all these minerals and no DIC loss was expected (Tab. 2). However, upon addition of HgCl<sub>2</sub> or  
475 CuCl<sub>2</sub>, some carbonate minerals, e.g., HgCO<sub>3</sub> or malachite and azurite, respectively, were expected to  
476 spontaneously precipitate given their relatively high saturation index values.

477 **Table 2.** pH and saturation indices of selected carbonate minerals estimated by PHREEQC for the  
478 unpreserved and preserved samples

Preservatives	pH	Saturation indices			
		HgCO <sub>3</sub>	Cu <sub>2</sub> (OH) <sub>2</sub> CO <sub>3</sub> - Malachite	Cu <sub>2</sub> (OH) <sub>2</sub> CO <sub>3</sub> - Azurite	Ag <sub>2</sub> CO <sub>3</sub>
Unfixed	6.72	-2.31	-4.96	-8.71	-16.42
HgCl <sub>2</sub>	6.40	3.64	-5.89	-10.10	-17.20
CuCl <sub>2</sub>	6.45	-2.55	2.26	2.11	-17.44
AgNO <sub>3</sub>	6.71	-2.31	-4.97	-8.73	-4.33

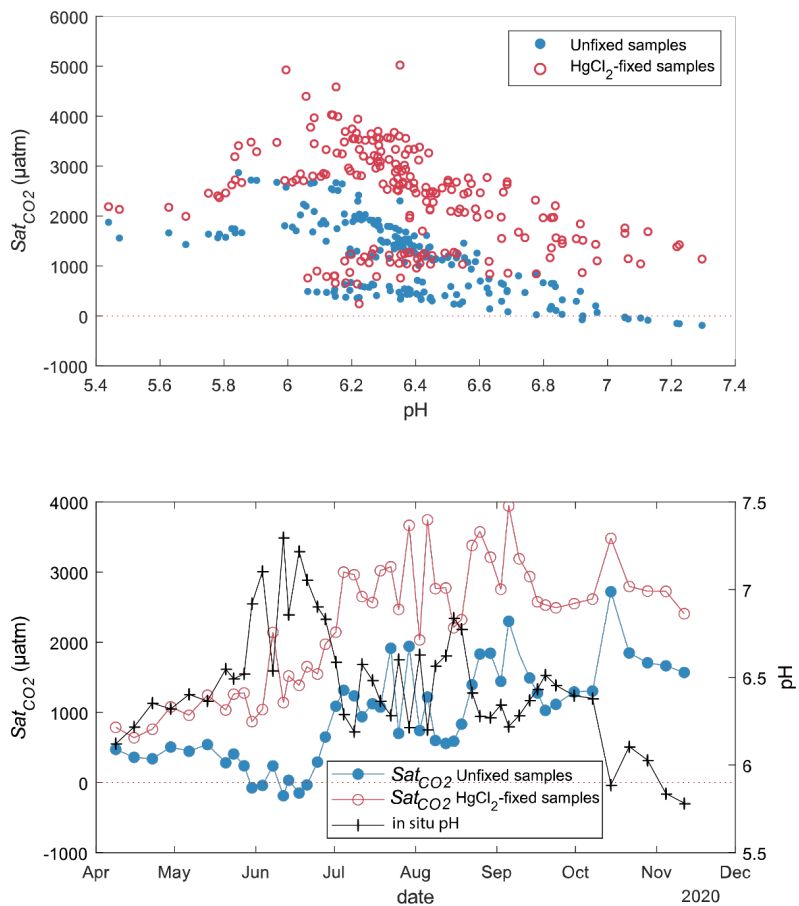
479

480 3.3. Effects of HgCl<sub>2</sub> on dissolved CO<sub>2</sub> concentration under a range of pH

481 CO<sub>2</sub> concentrations in unfixed water samples from Lake Lundebyvannet were significantly lower than  
482 in the HgCl<sub>2</sub>-fixed samples (mean difference: 52 μM; paired t-test; P<0.0001; Tab. 3). Fixation with  
483 HgCl<sub>2</sub> caused a general overestimation of CO<sub>2</sub> concentration and the saturation deficit (Fig. 34), thus  
484 missing out events of CO<sub>2</sub> influx (carbon sink) under high photosynthesis activity (high pH; Fig. 34).  
485 In parallel, PHREEQC predicted a decrease of 0.6 to 1.8 units of pH related to HgCl<sub>2</sub> addition (Fig.  
486 S1).

487

CO<sub>2</sub> overestimation from HgCl<sub>2</sub> fixation – Clayer et al.



488

489 **Figure 43.** CO<sub>2</sub> saturation deficit ( $Sat_{CO_2}$ ) in Lake Lundebyvannet as a function of in situ pH for all  
490 unfixed (obtained from DIC analysis) and HgCl<sub>2</sub>-fixed (obtained from GC analysis) samples (top  
491 panel). Timeseries of pH and CO<sub>2</sub> saturation deficit of surface water (1-m deep) for unfixed and  
492 HgCl<sub>2</sub>-fixed samples (bottom panel).

CO<sub>2</sub> overestimation from HgCl<sub>2</sub> fixation – Clayer et al.

493 **Table 3.** CO<sub>2</sub> concentrations ([CO<sub>2</sub>], μM) and diffusion fluxes (F<sub>CO<sub>2</sub></sub>, mol m<sup>-2</sup> d<sup>-1</sup>) from Lake  
 494 Lundebyvannet estimated from HgCl<sub>2</sub>-fixed and unfixed samples following Cole and Caraco (1998).  
 495 Ice-free season spans April to November. Data are also shown in Fig. 56.

Preservatives		Apr.	May	Jun.	Jul.	Aug.	Sep.	Oct.	Nov.	Ice-free season
[CO <sub>2</sub> ]	None	45	39	19	68	59	85	123	120	67
	HgCl <sub>2</sub>	68	75	74	133	130	149	179	178	121
	Diff (%)	+50	+93	+296	+96	+119	+75	+45	+49	+82
F <sub>CO<sub>2</sub></sub>	None	0.10	0.07	0.01	0.15	0.11	0.23	0.37	0.48	0.17
	HgCl <sub>2</sub>	0.20	0.21	0.16	0.34	0.29	0.47	0.57	0.77	0.35
	Diff (%)	+97	+188	+2163	+130	+162	+99	+55	+62	+108

496 The pH value of water samples from Lake Lundebyvannet varied between 5.4 and 7.3 (Fig 3-4 and  
 497 45), mainly due to marked variations in phytoplankton photosynthetic activity (Rohrlack et al., 2020).  
 498 The relative overestimation of CO<sub>2</sub> (*E*) follows an exponential increase with pH and is well  
 499 reproduced by a simple exponential function ( $2.56 \times 10^{-5} \times 10^{1.015 \times pH}$ , RMSE=44%, R<sup>2</sup>=0.81,  
 500 p<0.0001; Fig. 45).

501

## 502 4. Discussion

503 Prior to using dissolved gas concentrations in freshwater to estimate the magnitude of biological  
 504 aquatic processes such as photosynthesis and oxic respiration, denitrification and methanogenesis, we  
 505 must ensure that biological activity between sampling and laboratory analyses was efficiently  
 506 inhibited without significant impacts on the sample's chemistry. Here we report a unique dataset on  
 507 the impact of three preservatives on water samples from a typical low-ionic strength, unproductive  
 508 boreal lake to inform on potential risks of mis-estimation of dissolved gas concentrations. We further  
 509 show, using CO<sub>2</sub> concentration data from a typical productive boreal lake, that using HgCl<sub>2</sub> can lead  
 510 to negligence of the role of photosynthesis in lake C cycling.

### 511 4.1 Best preservative for the determination of dissolved gas concentrations

512 Given that none of the four treatments (unfixed, HgCl<sub>2</sub>, CuCl<sub>2</sub> or AgNO<sub>3</sub>) applied to Lake Svartkulp  
 513 water samples during the 3-month incubation offer an independent control, a first challenge is to  
 514 determine which of the treatment represent the most realistic dissolved gas concentrations close to  
 515 real condition. For CO<sub>2</sub> and O<sub>2</sub>, a few studies have used unfixed samples (only preserved dark at  
 516 +4°C) up to 48h after sampling to determine CO<sub>2</sub> or DIC concentrations (e.g., Sobek et al. 2003,  
 517 Kokic et al., 2015). So, the CO<sub>2</sub> and O<sub>2</sub> concentrations in the unfixed samples collected after 24h  
 518 incubation are the most representative of the initial real concentrations. Biological activity might have

519 had an impact, but this is likely negligible over the first 24h. In addition, the fact that the CO<sub>2</sub> and O<sub>2</sub>  
520 concentrations in the samples fixed with AgNO<sub>3</sub> after 24h, three weeks and three months are equal to  
521 those from unfixed samples after 24h (Fig. 42) confirms that the unfixed samples after 24h can be  
522 used as a control. In fact, only samples fixed with AgNO<sub>3</sub> are trustful given the expected toxicity of  
523 Ag, the absence of impact on pH (Fig. 23), and unchanged concentrations over the three-month  
524 experiment for all gases. Similarly, N<sub>2</sub>O and N<sub>2</sub> concentrations in the unfixed samples after 24h can  
525 be used as control. However, for CH<sub>4</sub>, Fig. 42 shows that already after 24h, the CH<sub>4</sub> concentration in  
526 the unfixed samples is below atmospheric saturation while it is consistently much higher in all three  
527 sets of fixed samples. Boreal lakes are typically over saturated with respect to CH<sub>4</sub> (Valiente et al.,  
528 2022) and it is very unlikely that CH<sub>4</sub> could have been produced in lake water incubated under high  
529 concentration of oxygen and toxic preservatives. Hence, unfixed samples do not represent real CH<sub>4</sub>  
530 concentrations. These observations are all consistent with the fact that the three preservatives were  
531 effective in preserving CH<sub>4</sub> from oxidation. Even ~~at~~ ~~over~~ 24h, preservatives need to be added to  
532 oxic water samples to are required to preserve CH<sub>4</sub> in oxic samples from oxidation. In fact, oxic  
533 methanotrophy typically show rates in the order of  $\mu\text{M day}^{-1}$  (Thottathil et al., 2019; van Grinsven et  
534 al., 2021). Hence, a CH<sub>4</sub> consumption of 0.3  $\mu\text{M}$  within 24h in the unfixed water samples is realistic  
535 (Fig. 42).

536 In summary, preservation with AgNO<sub>3</sub> is the only method that offered robust determination of all five  
537 dissolved gases with negligible changes in concentration over time.

#### 538 4.2 Risks of mis-estimating dissolved gas concentration with HgCl<sub>2</sub> and CuCl<sub>2</sub> preservation

539 Both sets of samples preserved with either HgCl<sub>2</sub> and CuCl<sub>2</sub> showed CO<sub>2</sub> concentrations that were  
540 much higher than ~~the~~ the unfixed (after 24h) or the AgNO<sub>3</sub>-fixed samples. This is due to an acidification  
541 of the poorly buffered (alkalinity 127  $\mu\text{M}$ ) and near neutral water (pH=6.73), shifting the carbonate  
542 equilibrium from HCO<sub>3</sub> to CO<sub>2</sub> as also shown by Borges et al. (2019). In fact, a rapid decrease in pH  
543 was observed upon HgCl<sub>2</sub> and CuCl<sub>2</sub> ~~amendments-treatments~~ (Fig. 23). The increase of CO<sub>2</sub> from  
544 about 130  $\mu\text{M}$  to  $\sim 160$   $\mu\text{M}$  after 3 weeks in both sample sets preserved with HgCl<sub>2</sub> and CuCl<sub>2</sub> is not  
545 mirrored by a similar decrease in O<sub>2</sub> (Fig. 42). This suggests that oxic respiration is not the main  
546 source for this additional 30  $\mu\text{M}$  of CO<sub>2</sub> but rather points towards additional acidification of the  
547 samples caused, e.g., by kinetically controlled complexation of Hg<sup>2+</sup> with dissolved organic matter  
548 (Miller et al., 2009). In fact, the relatively slow complexation of Hg<sup>2+</sup> with organic thiol groups can  
549 release two protons (Skylberg, 2008) and up to three, with some participation of a third weak-acid  
550 group (Khwaja et al., 2006). The transient nature of acidification caused by HgCl<sub>2</sub> and CuCl<sub>2</sub> is also  
551 evident in the pH impacts showing higher acidification after 24h than after 2h incubation (Fig. 23).  
552 The following decrease in CO<sub>2</sub> after 3 months (down to  $\sim 145$   $\mu\text{M}$ ) points to other processes. The  
553 precipitation of Hg and Cu carbonates, given their high saturation index values (Tab. 2), would be

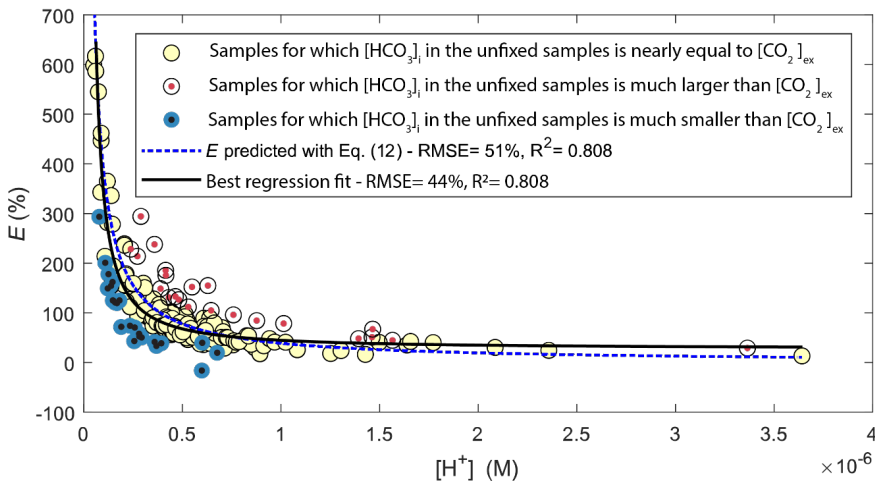
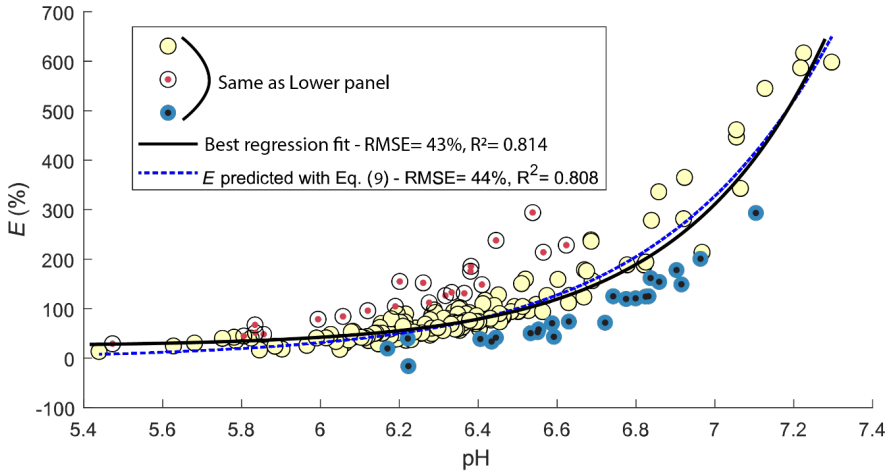
CO<sub>2</sub> overestimation from HgCl<sub>2</sub> fixation – Clayer et al.

554 consistent with the decrease in CO<sub>2</sub> concentrations observed between three weeks and three months.  
555 Calcite precipitation is typically observed in supersaturated solutions within 48h (Kim et al., 2020).  
556 Hence, it is realistic to consider that Hg and Cu carbonate precipitation influenced the CO<sub>2</sub>  
557 concentration within the preserved samples over the three months of storage time. Impacts of Hg or  
558 Cu carbonate precipitation is not evident after three weeks likely because of slow but persistent CO<sub>2</sub>  
559 production in presence of HgCl<sub>2</sub> and CuCl<sub>2</sub> related to acidification as described above (Fig. 42).  
560 However, after three weeks, this production likely weakens and is counterbalanced by increasing  
561 carbonate precipitation.

562 Overall, the addition of HgCl<sub>2</sub> or CuCl<sub>2</sub> following sampling increased CO<sub>2</sub> concentrations by 47%  
563 within the first 24h compared to the unfixed consistent with the -0.16 to -0.21 pH-unit acidification  
564 observed over the same time in the pH incubation experiment (Fig. 23) and the pH estimated with  
565 PHREEQC without the interaction with dissolved organic matter (Tab. 2). In fact, introducing pH and  
566 CO<sub>2</sub> concentration values of 6.40–6.45 and 130 μM, respectively, for the samples preserved with  
567 HgCl<sub>2</sub> and CuCl<sub>2</sub> into Eqs. 1 and 2 yields DIC concentrations (C<sub>T</sub>) of about 270 μM at t=24h. These  
568 DIC concentrations are almost equal to those calculated for the unfixed samples and those preserved  
569 with AgNO<sub>3</sub> at t = 24h, i.e., with a pH of 6.73 and CO<sub>2</sub> concentration of 88 μM. Interestingly, the  
570 concentration of CO<sub>2</sub> in the samples preserved with HgCl<sub>2</sub> and CuCl<sub>2</sub> continues to increase up to ~160  
571 μM after 3 weeks. Given that oxic respiration is inhibited (Fig. 42), this additional CO<sub>2</sub> is believed to  
572 originate from progressive release of protons following relatively slow complexation of Hg<sup>2+</sup> with  
573 dissolved organic matter (Khawaja et al., 2006; Miller et al., 2009; Skyllberg, 2008). Note however  
574 that this process could not be predicted with PHREEQC could not predict complexation of Hg<sup>2+</sup> with  
575 dissolved organic matter given that we it neglected the effect of dissolved organic matter.

576 Unlike the AgNO<sub>3</sub>-fixed samples, all the other samples showed an initial increase in N<sub>2</sub>O  
577 concentration from 24h to 3 weeks, followed by a decrease from three weeks to 3 months. Similar  
578 patterns of net N<sub>2</sub>O production followed by net consumption were also reported in short-term  
579 incubations of seawater from the high latitude Atlantic Ocean, although over much shorter timescales,  
580 i.e., 48 and 96h (Rees et al., 2021). The large difference in kinetics between the latter experiment  
581 (Rees et al., 2021) and our incubation might be attributable to differences in incubation temperature  
582 where the seawater from the high latitude Atlantic Ocean was incubated at ambient temperatures  
583 while our samples were kept at +4°C. Other difference in the experimental setup might have also  
584 played a role. The lack of inhibition of N<sub>2</sub>O production and consumption in the samples preserved  
585 with HgCl<sub>2</sub> and CuCl<sub>2</sub> can be attributed to the fact that N<sub>2</sub>O production tends to increase under  
586 increasing acidic conditions (Knowles, 1982; Mørkved et al., 2007; Seitzinger, 1988). In fact, the  
587 mole fraction of N<sub>2</sub>O produced during denitrification increases compared to N<sub>2</sub> as pH decreases  
588 (Knowles, 1982).

589



590

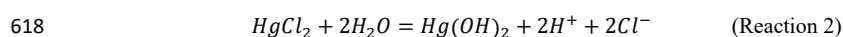
591 **Figure 45.** Comparison of observed (circles) and predicted (blue line) relative overestimation ( $E$ ) of  
 592 CO<sub>2</sub> concentrations caused by HgCl<sub>2</sub> fixation in Lake Lundebyvannet samples as a function of pH  
 593 (top panel) or proton concentration (bottom panel). The black line shows the best fit of the regression  
 594 analysis. White symbols represent samples for which the bicarbonate concentration in the unfixed  
 595 samples ( $[HCO_3^-]_i$ ) is nearly equal to CO<sub>2</sub> overestimation ( $[CO_2]_{ex}$ ), i.e.,  $\pm 20\mu M$  (equivalent to a pH  
 596 error of 0.05), while red and blue symbols represent samples for which initial bicarbonate  
 597 concentration was lower and higher than the CO<sub>2</sub> overestimation, respectively.

598 4.3 Using PHREEQC to estimate acidification caused by HgCl<sub>2</sub> in samples from Lake Lundebyvannet

599 As for the samples from Lake Svartkulp as described above, the overestimation of CO<sub>2</sub> concentration  
 600 in the samples from Lake Lundebyvannet fixed with HgCl<sub>2</sub> (161 μM added; Fig. 34) likely stems  
 601 from the acidification shifting the carbonate equilibrium from bicarbonate to CO<sub>2</sub>. In fact, PHREEQC  
 602 predicted a decrease of 0.6 to 1.8 units of pH related to HgCl<sub>2</sub> addition in these samples (Fig. S1).

603 The relative overestimation of CO<sub>2</sub> (*E* in Fig. 45) followed a typical exponential increase reflecting  
 604 the decrease in absolute CO<sub>2</sub> concentration with increasing pH (Stumm & Morgan, 1981) caused here  
 605 by phytoplankton photosynthesis. In fact, the exponential increase in CO<sub>2</sub> overestimation is easily  
 606 predicted by Eq. (9) with an equivalent level of accuracy as the optimized exponential function (Fig.  
 607 45). Consistently, the relative overestimation of CO<sub>2</sub> (*E*) shows an inverse decrease with [H<sup>+</sup>] that is  
 608 well reproduced by a simple inverse function ( $3.25 \times 10^{-5} / [H^+]$ ; RMSE=44%, R<sup>2</sup>=0.81, p<0.0001;  
 609 Fig. 45) and predicted by Eq. (15), with an α value of 1. Combining Eqs. 8 and 15 and solving it with  
 610 pH values estimated from PHREEQC (Fig. S1) for α yields values ranging between 0.72 and 0.89  
 611 with an average of 0.85. Unexpectedly, this average α value is almost equal to the ratio of the inverse  
 612 function coefficient and K<sub>1</sub>, i.e.,  $\frac{3.25 \times 10^{-5}}{K_1} = 0.87$ . Hence, the relative overestimation of CO<sub>2</sub> (*E*)  
 613 caused by HgCl<sub>2</sub> fixation is easily predicted by the change in bicarbonate equilibrium knowing the  
 614 proton release from HgCl<sub>2</sub> addition, here estimated with PHREEQC.

615 Hence, PHREEQC can be used to predict decrease in pH caused by HgCl<sub>2</sub> fixation, if sufficient  
 616 knowledge is gathered on the ionic water composition. Proton release during HgCl<sub>2</sub> fixation can be  
 617 represented by the following reaction:



619 From reaction 2, it becomes evident that the initial concentration of chloride in the water samples will  
 620 likely limit HgCl<sub>2</sub> dissociation and proton release. This is a likely mechanism occurring in seawater  
 621 where HgCl<sub>2</sub> has been shown to cause a decrease in pH, although at a negligible level with a  
 622 maximum decrease in pH of -0.01 (Chou et al., 2016).

623 Figure 3 shows that a range of water samples were associated with a relative CO<sub>2</sub> overestimation (*E*)  
 624 that substantially deviated from the overestimation predicted with Eq. 12 (red and blue symbols in  
 625 Fig. 45). In fact, some samples had a higher initial bicarbonate content ([HCO<sub>3</sub><sup>-</sup>]<sub>i</sub>) than the excess  
 626 CO<sub>2</sub> concentration ([CO<sub>2</sub>]<sub>ex</sub>), while other showed the opposite. The former case (blue symbols in Fig.  
 627 45) can easily be explained by a higher buffering capacity of the sampled water, i.e., a higher pH after  
 628 HgCl<sub>2</sub>-fixation than that predicted by PHREEQC related to a different water composition. Indeed, the  
 629 concentration of major elements in the water from Lake Lundebyvannet may vary significantly over  
 630 time, and in absence of data, we considered that the water composition, except for DIC, pH and



CO<sub>2</sub> overestimation from HgCl<sub>2</sub> fixation – Clayer et al.

631 HgCl<sub>2</sub>, was constant over time. By contrast, samples associated with  $[CO_2]_{ex}$  being larger than  
632  $[HCO_3^-]_i$  are more enigmatic. In order to shed light on possible explanations, we visually inspected  
633 trends between empirical deviations from predictions, i.e., residuals, and *in situ* temperature or pH.  
634 Absolute values of residuals showed a progressive increase with pH and *in situ* temperature which is  
635 in agreement with decreasing precision of the headspace method with increasing temperature and pH  
636 (Koschorreck et al., 2021). In fact, CO<sub>2</sub> is less soluble at higher temperature, hence more gas can  
637 evade during sampling, and thus the error increases with *in situ* temperature. In addition, at higher pH,  
638 CO<sub>2</sub> concentration decreases and consequently the absolute error on CO<sub>2</sub> quantification becomes  
639 larger relative to measured CO<sub>2</sub> concentration. Interestingly, many of the high residual values were  
640 not evenly distributed across the year, nor across the summer and were rather associated with only a  
641 few specific sampling events during summer (Fig. S2). This suggests that degassing could have  
642 occurred due to high ambient temperature in the field. Water associated with  $[CO_2]_{ex}$  being larger  
643 than  $[HCO_3^-]_i$  (red symbols in Fig. 4-5 and S4) could have been subject to a larger degassing in the  
644 samples collected for DIC analysis than the samples for GC analysis. On the other hand, degassing  
645 was likely larger for samples for GC analysis than for DIC analysis for water associated with  
646  $[HCO_3^-]_i$  being larger than  $[CO_2]_{ex}$  (blue symbols in Fig. 4-5 and Fig. S2). In addition to degassing  
647 and temperature effects, errors in pH measurements can also cause a large misestimation of CO<sub>2</sub>  
648 concentration from DIC analysis, and this error increases exponentially with pH following the shift in  
649 carbonate equilibrium. In summary, our analysis is consistent with that of Koschorreck et al. (2021)  
650 showing that errors in the determination of CO<sub>2</sub> concentrations are smaller at lower pH and lower  
651 temperature (Fig. S2).

#### 652 4.4. Implications for the estimation of lake and reservoir C cycling and recommendations

653 Using HgCl<sub>2</sub> or CuCl<sub>2</sub> to preserve dissolved gas samples in poorly buffered water samples has large  
654 impacts on CO<sub>2</sub> concentrations with considerable risk of leading to incorrect interpretations. The risk  
655 of mis-estimating CO<sub>2</sub> concentration due to HgCl<sub>2</sub> and CuCl<sub>2</sub> preservation is the highest when ~~natural~~  
656 ~~water~~ pH of the unfixed water is close to the first carbonic acid dissociation constant ( $pK_1 = 6.41$  at  
657 25°C; Stumm & Morgan, 1996). It implies that any small shift in pH will have a significant impact in  
658 the carbonate equilibrium between bicarbonate to CO<sub>2</sub>. The risk is also the highest in the lowest ionic  
659 strength waters. In that respect, low-ionic strength, slightly acidic to neutral, moderately humic lakes  
660 commonly found in Norway (de Wit et al., 2023), large parts of Sweden (Valina et al. 2014), and  
661 Finland, Atlantic Canada (Houle et al., 2022), Ontario, Québec, and North-East USA (Skjelkvåle and  
662 de Wit 2011; Weyhenmeyer et al., 2019) are the most prone to errors in CO<sub>2</sub> concentrations related to  
663 HgCl<sub>2</sub> or CuCl<sub>2</sub> preservation. Through a preliminary literature search we found several studies from  
664 boreal lakes (Jonsson et al., 2001; Urabe et al., 2011; Yang et al., 2015; Hessen et al., 2017) but also  
665 from circum-neutral pH sub-tropical to tropical aquatic environments (Jeffrey et al., 2018; Webb et  
666 al., 2018; Ray et al., 2021) where preservation with HgCl<sub>2</sub> may have caused biases in the

Formatted: Subscript

667 [quantification of CO<sub>2</sub> concentrations as it was the case for samples from the Congo River \(Borges et](#)  
668 [al., 2019\)](#). A significant part of these low-ionic strength [boreal](#) lakes become increasingly sensitive to  
669 changes in nutrients with strong impacts on their role in carbon cycling (Myrstener et al., 2022). In  
670 this context, it is crucial to avoid mis-estimation of CO<sub>2</sub> concentrations and thus avoid use of HgCl<sub>2</sub> or  
671 CuCl<sub>2</sub> to ensure a robust understanding of the role of autotrophic processes in lake C cycling. Below  
672 we describe the implications for the lake C budget of Lundebyvannet as an example of a mis-  
673 estimation of the role of photosynthesis in a typical productive boreal lake.

674 In Lake Lundebyvannet, over the ice-free season, average CO<sub>2</sub> concentrations determined following  
675 HgCl<sub>2</sub>-fixation and GC analysis were 82% higher than those obtained from DIC analyses (Tab. 3; Fig.  
676 [5-6](#) and S3). CO<sub>2</sub> concentrations obtained from HgCl<sub>2</sub>-fixed samples created the illusion that Lake  
677 Lundebyvannet was a steady net source of CO<sub>2</sub> to the atmosphere over the ice-free season with large  
678 CO<sub>2</sub> saturation deficit (Fig. [34](#)) while, in reality, the lake switched from being a net source in May, to  
679 a net sink over a few weeks in June, and returning to a net source in July (Fig. [5-6](#) and S3). Indeed,  
680 monthly CO<sub>2</sub> overestimation related to HgCl<sub>2</sub>-fixation reached about 300% in June (Tab. 3).  
681 Propagating this overestimation into the estimates of CO<sub>2</sub> diffusion fluxes with typical wind-based  
682 models yields overestimation of CO<sub>2</sub> fluxes of 108–112% over the ice-free season and up to 2100% in  
683 June (Tab. 3 and S3). Hence, interpreting CO<sub>2</sub> data without correcting for CO<sub>2</sub> overestimation caused  
684 by HgCl<sub>2</sub>-fixation leads to negligence of the role of photosynthesis in lake C cycling with major  
685 implications for current and future predictions of lake CO<sub>2</sub> emissions.

686 The use of HgCl<sub>2</sub> to preserve water samples prior to dissolved gas analyses is part of the current  
687 guidelines for greenhouse gas measurements in freshwater reservoirs (Machado Damazio et al., 2012;  
688 UNESCO/IHA, 2008, 2010). Hence, there is a risk of overestimating CO<sub>2</sub> concentrations and  
689 emissions, in absence of discrete measurement of emissions, from hydropower reservoirs with  
690 consequence on the present and expected greenhouse gas footprint from hydroelectricity. To ensure  
691 precise estimation of greenhouse [gas](#) concentration and, possibly, emission from hydropower, the use  
692 of HgCl<sub>2</sub> should therefore be discontinued.

## 693 5. Conclusion

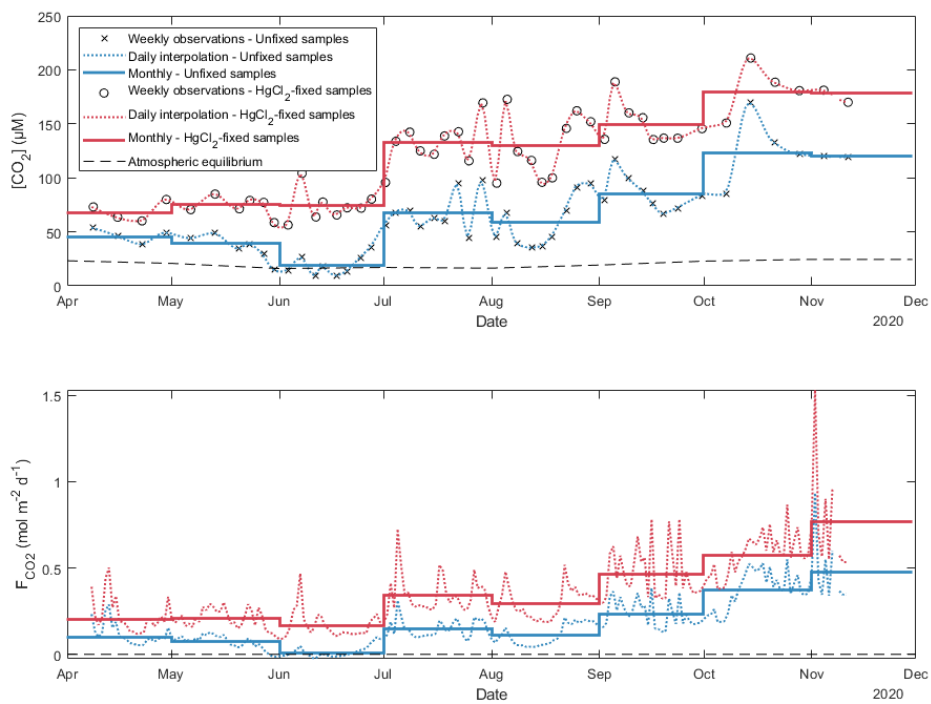
694 Mercury is a potent neurotoxin for humans and toxic for the environment and its use should be  
695 discouraged, notably following the Minamata convention on mercury, a global treaty ratified by 126  
696 countries (16 December 2020) to protect human health and the environment from the adverse effects  
697 of mercury. This study further questions the use of HgCl<sub>2</sub> for preservation of poorly buffered (low  
698 ionic strength) water samples with high DOC concentration for analysis of dissolved gases in the  
699 laboratory. Although CuCl<sub>2</sub> is less toxic, it behaved similarly to HgCl<sub>2</sub> and cannot be recommend. In  
700 fact, both chlorinated inhibitors caused a significant decrease in pH shifting the carbonate equilibrium  
701 towards CO<sub>2</sub> and are also suspected to promote carbonate precipitation over long-term storage. The

Formatted: Subscript

CO<sub>2</sub> overestimation from HgCl<sub>2</sub> fixation – Clayer et al.

702 only promising inhibitor tested in this study was AgNO<sub>3</sub> notably for dissolved CO<sub>2</sub>, CH<sub>4</sub> and N<sub>2</sub>O.  
703 Silver nitrate is a suitable substitute for HgCl<sub>2</sub> in low-ionic strength waters, further tests should be  
704 carried out with a range of inhibitor concentration and more diverse water samples. The use of  
705 chemical inhibitors may not be the best approach. Alternatives exist, such as directly measuring gas  
706 concentrations *in situ* with sensors, or sampling the headspace out in the field, and bringing back gas  
707 samples (e.g., Cole et al., 1994; Karlsson et al., 2013; Kling et al., 1991; Valiente et al., 2022), rather  
708 than water samples, to the lab for gas chromatography analyses. However, care must be taken to know  
709 the exact equilibration temperature (Koschorreck et al., 2021) and to avoid gas exchange with the  
710 atmosphere as well as to use a clean background gas during headspace equilibration which can be  
711 challenging in remote environments under harsh meteorological conditions.

CO<sub>2</sub> overestimation from HgCl<sub>2</sub> fixation – Clayer et al.



712

713 **Figure 56.** Daily and monthly surface CO<sub>2</sub> concentrations ([CO<sub>2</sub>]; top panel) and diffusion fluxes  
714 (F<sub>CO<sub>2</sub></sub>; bottom panel) at the water-atmosphere interface from Lake Lundebyvannet (also in Tab. 3).  
715 Unfixed samples were obtained by DIC analysis. Daily [CO<sub>2</sub>] was interpolated from weekly data  
716 using a modified spline (see text for details). Diffusion fluxes were calculated following Cole &  
717 Caraco (1998).

CO<sub>2</sub> overestimation from HgCl<sub>2</sub> fixation – Clayer et al.

718 We further advise against interpretation of CO<sub>2</sub> concentration data from low ionic strength, circum-  
719 neutral water samples preserved with HgCl<sub>2</sub> or CuCl<sub>2</sub>. The overestimation of CO<sub>2</sub> concentration  
720 caused by HgCl<sub>2</sub> can mask the effect of photosynthesis on lake carbon balance, creating the illusion  
721 that lakes are net CO<sub>2</sub> sources when they are net CO<sub>2</sub> sinks. Our analysis from Lake Lundebyvannet  
722 shows that HgCl<sub>2</sub> fixation led to an overestimation of the CO<sub>2</sub> concentration by a factor of 1.8, on  
723 average, but approaching a factor of 4 during the peak photosynthetic period. An even larger impact is  
724 expected on CO<sub>2</sub> diffusive fluxes which were overestimated by a factor of 2 on average and up to a  
725 factor of >20 during peak photosynthesis. Interpreting such data would have underestimated the  
726 current and future role of aquatic photosynthesis.

#### 727 **Data availability**

728 All data supporting this study will be made available on a permanent repository upon acceptance, e.g.,  
729 Hydroshare.

#### 730 **Author contribution**

731 JET, AK, and TR supervised and PD, KN and FC contributed to the study design. JET, KN and TR  
732 carried out the experiments. PD and TR performed the chemical analyses. JET and FC wrote the first  
733 draft. FC performed the modelling, data, and statistical analyses, and drafted the figures. All co-  
734 authors edited the manuscript.

#### 735 **Competing interests**

736 The contact author has declared that none of the authors has any competing interests.

#### 737 **Acknowledgements**

738 We are grateful to Benoît Demars for research assistance, coordination, and useful comments and  
739 discussions on an earlier version of this manuscript and to Heleen de Wit for discussions. Research  
740 was funded by NIVA and through the Global Change at Northern Latitude (NoLa) project #200033.

741

#### 742 **References**

- 743 Akima, H. (1974). A method of bivariate interpolation and smooth surface fitting based on local  
744 procedures. *Communications of the ACM*, 17(1), 18–20.  
745 <https://doi.org/10.1145/360767.360779>
- 746 Allison, J., Brown, D., & Novo-Gradac, K. (1991). *MINTEQA2/PRODEFA2, a geochemical*  
747 *assessment model for environmental systems: Version 3. 0 user's manual*. GA: US  
748 Environmental Protection Agency.
- 749 Amorim, M. J. B., & Scott-Fordsmand, J. J. (2012). Toxicity of copper nanoparticles and CuCl<sub>2</sub> salt  
750 to *Enchytraeus albidus* worms: Survival, reproduction and avoidance responses.  
751 *Environmental Pollution*, 164, 164–168. <https://doi.org/10.1016/j.envpol.2012.01.015>

- 752 [Atekwana, E. A., Molwalefhe, L., Kgaodi, O., & Cruse, A. M. \(2016\). Effect of evapotranspiration on](#)  
 753 [dissolved inorganic carbon and stable carbon isotopic evolution in rivers in semi-arid](#)  
 754 [climates: The Okavango Delta in North West Botswana. \*Journal of Hydrology: Regional\*](#)  
 755 [Studies, 7, 1–13. <https://doi.org/10.1016/j.ejrh.2016.05.003>](#)  
 756 [Borges, A. V., Darchambeau, F., Lambert, T., Morana, C., Allen, G. H., Tambwe, E., Toengaho](#)  
 757 [Sembaito, A., Mambo, T., Nlandu Wabakhangazi, J., Descy, J.-P., Teodoru, C. R., &](#)  
 758 [Bouillon, S. \(2019\). Variations in dissolved greenhouse gases \(CO<sub>2</sub>, CH<sub>4</sub>, N<sub>2</sub>O\) in the Congo](#)  
 759 [River network overwhelmingly driven by fluvial-wetland connectivity. \*Biogeosciences\*,](#)  
 760 [16\(19\), 3801–3834. <https://doi.org/10.5194/bg-16-3801-2019>](#)  
 761 [Carroll J.J., Slupsky J.D. & Mather A.E. \(1991\) The solubility of carbon dioxide in water at low](#)  
 762 [pressure. \*Journal of Physical and Chemical Reference Data\*, 20, 1201-1209.](#)  
 763 [https://doi.org/10.1063/1.555900](#)  
 764 [Chen, C. Y., Driscoll, C., Eagles-Smith, C. A., Eckley, C. S., Gay, D. A., Hsu-Kim, H., Keane, S. E.,](#)  
 765 [Kirk, J. L., Mason, R. P., Obrist, D., Selin, H., Selin, N. E., & Thompson, M. R. \(2018\). A](#)  
 766 [Critical Time for Mercury Science to Inform Global Policy. \*Environmental Science &\*](#)  
 767 [Technology, 52\(17\), 9556–9561. <https://doi.org/10.1021/acs.est.8b02286>](#)  
 768 [Chen H., Johnston R.C., Mann B.F., Chu R.K., Tolic N., Parks J.M. & Gu B. \(2017\) Identification of](#)  
 769 [mercury and dissolved organic matter complexes using ultrahigh resolution mass](#)  
 770 [spectrometry. \*Environmental Science & Technology Letters\*, 4, 59-65.](#)  
 771 [https://doi.org/10.1021/acs.estlett.6b00460](#)  
 772 [Chou W.C., Gong G.C., Yang C.Y. & Chuang K.Y. \(2016\) A comparison between field and](#)  
 773 [laboratory pH measurements for seawater on the East China Sea shelf. \*Limnology and\*](#)  
 774 [Oceanography-Methods, 14, 315-322. <https://doi.org/10.1002/lom3.10091>](#)  
 775 [Ciavatta L. & Grimaldi M. \(1968\) The hydrolysis of mercury\(II\) chloride, HgCl<sub>2</sub>. \*Journal of\*](#)  
 776 [Inorganic and Nuclear Chemistry, 30, 563-581. \[https://doi.org/10.1016/0022-1902\\(68\\)80483-\]\(https://doi.org/10.1016/0022-1902\(68\)80483-X\)](#)  
 777 [X](#)  
 778 [Clayer, F., Gobeil, C., & Tessier, A. \(2016\). Rates and pathways of sedimentary organic matter](#)  
 779 [mineralization in two basins of a boreal lake: Emphasis on methanogenesis and](#)  
 780 [methanotrophy: Methane cycling in boreal lake sediments. \*Limnology and Oceanography\*,](#)  
 781 [61\(S1\), Article S1. <https://doi.org/10.1002/lno.10323>](#)  
 782 [Clayer, F., Thrane, J.-E., Brandt, U., Dörsch, P., & de Wit, H. A. \(2021\). Boreal Headwater](#)  
 783 [Catchment as Hot Spot of Carbon Processing From Headwater to Fjord. \*Journal of\*](#)  
 784 [Geophysical Research: Biogeosciences, 126\(12\), e2021JG006359.](#)  
 785 [https://doi.org/10.1029/2021JG006359](#)  
 786 [Cole, J. J., Caraco, N. F., Kling, G. W., & Kratz, T. K. \(1994\). Carbon Dioxide Supersaturation in the](#)  
 787 [Surface Waters of Lakes. \*Science\*, 265\(5178\), Article 5178.](#)  
 788 [https://doi.org/10.1126/science.265.5178.1568](#)  
 789 [Cole, J. J., & Caraco, N. F. \(1998\). Atmospheric exchange of carbon dioxide in a low-wind](#)  
 790 [oligotrophic lake measured by the addition of SF<sub>6</sub>. \*Limnology and Oceanography\*, 43\(4\),](#)  
 791 [Article 4. <https://doi.org/10.4319/lo.1998.43.4.0647>](#)  
 792 [Crusius, J., & Wanninkhof, R. \(2003\). Gas transfer velocities measured at low wind speed over a lake.](#)  
 793 [Limnology and Oceanography, 48\(3\), Article 3. <https://doi.org/10.4319/lo.2003.48.3.1010>](#)  
 794 [Deheyn, D. D., Bencheikh-Latmani, R., & Latz, M. I. \(2004\). Chemical speciation and toxicity of](#)  
 795 [metals assessed by three bioluminescence-based assays using marine organisms.](#)  
 796 [Environmental Toxicology, 19\(3\), 161–178. <https://doi.org/10.1002/tox.20009>](#)  
 797 [de Wit, H. A., Garmo, Ø. A., Jackson-Blake, L. A., Clayer, F., Vogt, R. D., Austnes, K., Kaste, Ø.,](#)  
 798 [Gundersen, C. B., Guerrero, J. L., & Hindar, A. \(2023\). Changing Water Chemistry in One](#)  
 799 [Thousand Norwegian Lakes During Three Decades of Cleaner Air and Climate Change.](#)  
 800 [Global Biogeochemical Cycles, 37\(2\), e2022GB007509.](#)  
 801 [https://doi.org/10.1029/2022GB007509](#)  
 802 [Dickson A.G., Sabine C.L. & Christian J.R. \(2007\) Guide to best practices for ocean CO<sub>2</sub>](#)  
 803 [measurements, North Pacific Marine Science Organization.](#)  
 804 [Duan, Z., & Mao, S. \(2006\). A thermodynamic model for calculating methane solubility, density and](#)  
 805 [gas phase composition of methane-bearing aqueous fluids from 273 to 523K and from 1 to](#)

Formatted: English (United States)

- 806 2000bar. *Geochimica et Cosmochimica Acta*, 70(13), Article 13.  
 807 <https://doi.org/10.1016/j.gca.2006.03.018>
- 808 Foti C., Giuffrè O., Lando G. & Sammartano S. (2009) Interaction of inorganic mercury (II) with  
 809 polyamines, polycarboxylates, and amino acids. *Journal of Chemical & Engineering Data*,  
 810 54, 893-903. <https://doi.org/10.1021/jc800685c>
- 811 Frost API. (2022). <https://frost.met.no/index.html>
- 812 [Golub, M., Desai, A. R., McKinley, G. A., Remucal, C. K., & Stanley, E. H. \(2017\). Large](#)  
 813 [Uncertainty in Estimating pCO<sub>2</sub> From Carbonate Equilibria in Lakes. \*Journal of Geophysical\*](#)  
 814 [Research: Biogeosciences, 122\(11\), 2909–2924. <https://doi.org/10.1002/2017JG003794>](#)
- 815 Guérin, F., Abril, G., Richard, S., Burbano, B., Reynouard, C., Seyler, P., & Delmas, R. (2006).  
 816 Methane and carbon dioxide emissions from tropical reservoirs: Significance of downstream  
 817 rivers. *Geophysical Research Letters*, 33(21). <https://doi.org/10.1029/2006GL027929>
- 818 Guérin, F., Abril, G., Serça, D., Delon, C., Richard, S., Delmas, R., Tremblay, A., & Varfalvy, L.  
 819 (2007). Gas transfer velocities of CO<sub>2</sub> and CH<sub>4</sub> in a tropical reservoir and its river  
 820 downstream. *Journal of Marine Systems*, 66(1), Article 1.  
 821 <https://doi.org/10.1016/j.jmarsys.2006.03.019>
- 822 Halmi, M. I. E., Kassim, A., & Shukor, M. Y. (2019). Assessment of heavy metal toxicity using a  
 823 luminescent bacterial test based on Photobacterium sp. Strain MIE. *Rendiconti Lincei. Scienze*  
 824 *Fisiche e Naturali*, 30(3), 589–601. <https://doi.org/10.1007/s12210-019-00809-5>
- 825 Hagman, C. H. C., Ballot, A., Hjermmann, D. Ø., Skjelbred, B., Brettum, P., & Ptacnik, R. (2015). The  
 826 occurrence and spread of Gonyostomum semen (Ehr.) Diesing (Raphidophyceae) in  
 827 Norwegian lakes. *Hydrobiologia*, 744(1), 1–14. <https://doi.org/10.1007/s10750-014-2050-y>
- 828 Hamme R.C. & Emerson S.R. (2004) The solubility of neon, nitrogen and argon in distilled water and  
 829 seawater. *Deep-Sea Research Part I-Oceanographic Research Papers*, 51, 1517-1528.  
 830 <https://doi.org/10.1016/j.dsr.2004.06.009>
- 831 Hassen A., Saidi N., Cherif M. & Boudabous A. (1998) Resistance of environmental bacteria to heavy  
 832 metals. *Bioresource technology*, 64, 7-15. [https://doi.org/10.1016/S0960-8524\(97\)00161-2](https://doi.org/10.1016/S0960-8524(97)00161-2)
- 833 Hessen, D. O., Håll, J. P., Thrane, J.-E., & Andersen, T. (2017). Coupling dissolved organic carbon,  
 834 CO<sub>2</sub> and productivity in boreal lakes. *Freshwater Biology*, 62(5), 945–953.  
 835 <https://doi.org/10.1111/fwb.12914>
- 836 Hilgert, S., Scapulatempo Fernandes, C. V., & Fuchs, S. (2019). Redistribution of methane emission  
 837 hot spots under drawdown conditions. *Science of The Total Environment*, 646, 958–971.  
 838 <https://doi.org/10.1016/j.scitotenv.2018.07.338>
- 839 Horvatić J. & Peršić V. (2007) The effect of Ni<sup>2+</sup>, Co<sup>2+</sup>, Zn<sup>2+</sup>, Cd<sup>2+</sup> and Hg<sup>2+</sup> on the growth  
 840 rate of marine diatom Phaeodactylum tricornutum Bohlin: microplate growth inhibition test.  
 841 *Bulletin of Environmental Contamination and Toxicology*, 79, 494-498.  
 842 <https://doi.org/10.1007/s00128-007-9291-7>
- 843 Houle, D., Augustin, F., & Couture, S. (2022). Rapid improvement of lake acid–base status in  
 844 Atlantic Canada following steep decline in precipitation acidity. *Canadian Journal of*  
 845 *Fisheries and Aquatic Sciences*, 79(12), 2126–2137. <https://doi.org/10.1139/cjfas-2021-0349>
- 846 IEA. (2020). *Key World Energy Statistics 2020*. IEA, International Energy Agency.  
 847 <https://www.iea.org/reports/key-world-energy-statistics-2020>
- 848 [Jeffrey, L. C., Santos, I. R., Tait, D. R., Makings, U., & Maher, D. T. \(2018\). Seasonal Drivers of](#)  
 849 [Carbon Dioxide Dynamics in a Hydrologically Modified Subtropical Tidal River and Estuary](#)  
 850 [\(Caboolture River, Australia\). \*Journal of Geophysical Research: Biogeosciences\*, 123\(6\),](#)  
 851 [1827–1849. <https://doi.org/10.1029/2017JG004023>](#)
- 852 [Jonsson, A., Meili, M., Bergström, A.-K., & Jansson, M. \(2001\). Whole-lake mineralization of](#)  
 853 [allochthonous and autochthonous organic carbon in a large humic lake \(örträsket, N.](#)  
 854 [Sweden\). \*Limnology and Oceanography\*, 46\(7\), 1691–1700.](#)  
 855 <https://doi.org/10.4319/lo.2001.46.7.1691>
- 856 [Karlsson, J., Giesler, R., Persson, J., & Lundin, E. \(2013\). High emission of carbon dioxide and](#)  
 857 [methane during ice thaw in high latitude lakes. \*Geophysical Research Letters\*, 40\(6\), Article](#)  
 858 [6. <https://doi.org/10.1002/grl.50152>](#)

- 859 Khwaja, A. R., Bloom, P. R., & Brezonik, P. L. (2006). Binding Constants of Divalent Mercury  
860 (Hg<sup>2+</sup>) in Soil Humic Acids and Soil Organic Matter. *Environmental Science & Technology*,  
861 40(3), 844–849. <https://doi.org/10.1021/es051085c>
- 862 Kim, D., Mahabadi, N., Jang, J., & van Paassen, L. A. (2020). Assessing the Kinetics and Pore-Scale  
863 Characteristics of Biological Calcium Carbonate Precipitation in Porous Media using a  
864 Microfluidic Chip Experiment. *Water Resources Research*, 56(2), e2019WR025420.  
865 <https://doi.org/10.1029/2019WR025420>
- 866 [Klaus, M. \(2023\). Decadal increase in groundwater inorganic carbon concentrations across Sweden.  
867 \*Communications Earth & Environment\*, 4\(1\), Article 1. \[https://doi.org/10.1038/s43247-023-  
868 00885-4\]\(https://doi.org/10.1038/s43247-023-00885-4\)](https://doi.org/10.1038/s43247-023-00885-4)
- 869 [Kling, G. W., Kipphut, G. W., & Miller, M. C. \(1991\). Arctic Lakes and Streams as Gas Conduits to  
870 the Atmosphere: Implications for Tundra Carbon Budgets. \*Science\*, 251\(4991\), 298–301.  
871 <https://doi.org/10.1126/science.251.4991.298>](https://doi.org/10.1126/science.251.4991.298)
- 872 Knowles, R. (1982). Denitrification. *Microbiological Reviews*, 46(1), 43–70.  
873 <https://doi.org/10.1128/mr.46.1.43-70.1982>
- 874 Kocik, J., Wallin, M. B., Chmiel, H. E., Denfeld, B. A., & Sobek, S. (2015). Carbon dioxide evasion  
875 from headwater systems strongly contributes to the total export of carbon from a small boreal  
876 lake catchment. *Journal of Geophysical Research: Biogeosciences*, 120(1), 13–28.  
877 <https://doi.org/10.1002/2014JG002706>
- 878 Koschorreck, M., Prairie, Y. T., Kim, J., & Marcé, R. (2021). Technical note: CO<sub>2</sub> is not like CH<sub>4</sub> –  
879 limits of and corrections to the headspace method to analyse pCO<sub>2</sub> in fresh water.  
880 *Biogeosciences*, 18(5), 1619–1627. <https://doi.org/10.5194/bg-18-1619-2021>
- 881 Larrañaga, M., Lewis, R., & Lewis, R. (2016). Hawley's Condensed Chemical Dictionary, Sixteenth  
882 Edition. i–xiii. <https://doi.org/10.1002/9781119312468.fmatter>
- 883 Liang X., Lu X., Zhao J., Liang L., Zeng E.Y. & Gu B. (2019) Stepwise reduction approach reveals  
884 mercury competitive binding and exchange reactions within natural organic matter and mixed  
885 organic ligands. *Environmental Science & Technology*, 53, 10685-10694.  
886 <https://doi.org/10.1021/acs.est.9b02586>
- 887 Machado Damazio, J., Cordeiro Geber de Melo, A., Piñeiro Maceira, M. E., Medeiros, A., Negrini,  
888 M., Alm, J., Schei, T. A., Tateda, Y., Smith, B., & Nielsen, N. (2012). *Guidelines for  
889 quantitative analysis of net GHG emissions from reservoirs: Volume 1: Measurement  
890 Programmes and Data Analysis*. International Energy Agency (IEA).  
891 [https://www.ieahydro.org/media/992f6848/GHG\\_Guidelines\\_22October2012\\_Final.pdf](https://www.ieahydro.org/media/992f6848/GHG_Guidelines_22October2012_Final.pdf)
- 892 Magen, C., Lapham, L. L., Pohlman, J. W., Marshall, K., Bosman, S., Casso, M., & Chanton, J. P.  
893 (2014). A simple headspace equilibration method for measuring dissolved methane.  
894 *Limnology and Oceanography: Methods*, 12(9), 637–650.  
895 <https://doi.org/10.4319/lom.2014.12.637>
- 896 Miller, C. L., Southworth, G., Brooks, S., Liang, L., & Gu, B. (2009). Kinetic Controls on the  
897 Complexation between Mercury and Dissolved Organic Matter in a Contaminated  
898 Environment. *Environmental Science & Technology*, 43(22), 8548–8553.  
899 <https://doi.org/10.1021/es901891t>
- 900 Millero F.J., Huang F. & Laferiere A.L. (2002) Solubility of oxygen in the major sea salts as a  
901 function of concentration and temperature. *Marine Chemistry*, 78, 217-230.  
902 [https://doi.org/10.1016/S0304-4203\(02\)00034-8](https://doi.org/10.1016/S0304-4203(02)00034-8)
- 903 Myrstener, M., Fork, M. L., Bergström, A.-K., Puts, I. C., Hauptmann, D., Isles, P. D. F., Burrows, R.  
904 M., & Sponseller, R. A. (2022). Resolving the Drivers of Algal Nutrient Limitation from  
905 Boreal to Arctic Lakes and Streams. *Ecosystems*, 25(8), 1682–1699.  
906 <https://doi.org/10.1007/s10021-022-00759-4>
- 907 Mørkved, P. T., Dörsch, P., & Bakken, L. R. (2007). The N<sub>2</sub>O product ratio of nitrification and its  
908 dependence on long-term changes in soil pH. *Soil Biology and Biochemistry*, 39(8), 2048–  
909 2057. <https://doi.org/10.1016/j.soilbio.2007.03.006>
- 910 NILU. (2022). *EBAS*. <https://ebas-data.nilu.no/Default.aspx>
- 911 Nowack, B., Krug, H. F., & Height, M. (2011). 120 Years of Nanosilver History: Implications for  
912 Policy Makers. *Environmental Science & Technology*, 45(4), 1177–1183.  
913 <https://doi.org/10.1021/es103316q>

Formatted: Norwegian (Bokmål)



- 914 NPIRS. (2023). *Purdue University*. <https://www.npirs.org/public>
- 915 Okuku, E. O., Bouillon, S., Tole, M., & Borges, A. V. (2019). Diffusive emissions of methane and  
 916 nitrous oxide from a cascade of tropical hydropower reservoirs in Kenya. *Lakes &*  
 917 *Reservoirs: Science, Policy and Management for Sustainable Use*, 24(2), 127–135.  
 918 <https://doi.org/10.1111/lre.12264>
- 919 Parkhurst, D. L., & Appelo, C. A. J. (2013). *Description of input and examples for PHREEQC version*  
 920 *3—A computer program for speciation, batch-reaction, one-dimensional transport, and*  
 921 *inverse geochemical calculations: U.S. Geological Survey Techniques and Methods* (book 6,  
 922 chap. A43; p. 497). USGS. <http://pubs.usgs.gov/tm/06/a43/>
- 923 Powell K.J., Brown P.L., Byrne R.H., Gajda T., Hefter G., Sjöberg S. & Wanner H. (2004) Chemical  
 924 speciation of Hg (II) with environmental inorganic ligands. *Australian Journal of Chemistry*,  
 925 **57**, 993-1000. <https://doi.org/10.1071/CH04063>
- 926 Rai L.C., Gaur J.P. & Kumar H.D. (1981) Phycology and heavy-metal pollution. *Biological Reviews*,  
 927 **56**, 99-151. <https://doi.org/10.1111/j.1469-185X.1981.tb00345.x>
- 928 Ratte, H. T. (1999). Bioaccumulation and toxicity of silver compounds: A review. *Environmental*  
 929 *Toxicology and Chemistry*, 18(1), 89–108. <https://doi.org/10.1002/etc.5620180112>
- 930 [Ray, R., Miyajima, T., Watanabe, A., Yoshikai, M., Ferrera, C. M., Orizar, I., Nakamura, T., San](#)  
 931 [Diego-McGlone, M. L., Herrera, E. C., & Nadaoka, K. \(2021\). Dissolved and particulate](#)  
 932 [carbon export from a tropical mangrove-dominated riverine system. \*Limnology and\*](#)  
 933 [Oceanography](#), 66(11), 3944–3962. <https://doi.org/10.1002/lno.11934>
- 934 Rees, A. P., Brown, I. J., Jayakumar, A., Lessin, G., Somerfield, P. J., & Ward, B. B. (2021).  
 935 Biological nitrous oxide consumption in oxygenated waters of the high latitude Atlantic  
 936 Ocean. *Communications Earth & Environment*, 2(1), Article 1.  
 937 <https://doi.org/10.1038/s43247-021-00104-y>
- 938 Rippner, D. A., Margenot, A. J., Fakra, S. C., Aguilera, L. A., Li, C., Sohng, J., Dynarski, K. A.,  
 939 Waterhouse, H., McElroy, N., Wade, J., Hind, S. R., Green, P. G., Peak, D., McElrone, A. J.,  
 940 Chen, N., Feng, R., Scow, K. M., & Parikh, S. J. (2021). Microbial response to copper oxide  
 941 nanoparticles in soils is controlled by land use rather than copper fate. *Environmental*  
 942 *Science: Nano*, 8(12), 3560–3576. <https://doi.org/10.1039/D1EN00656H>
- 943 Rohrlack T., Frostad P., Riise G. & Hagman C.H.C. (2020) Motile phytoplankton species such as  
 944 *Gonyostomum semen* can significantly reduce CO<sub>2</sub> emissions from boreal lakes.  
 945 *Limnologica*, **84**, 125810. <https://doi.org/10.1016/j.limno.2020.125810>
- 946 Schubert, C. J., Diem, T., & Eugster, W. (2012). Methane Emissions from a Small Wind Shielded  
 947 Lake Determined by Eddy Covariance, Flux Chambers, Anchored Funnels, and Boundary  
 948 Model Calculations: A Comparison. *Environmental Science & Technology*, 46(8), 4515–  
 949 4522. <https://doi.org/10.1021/es203465x>
- 950 Seitzinger, S. P. (1988). Denitrification in freshwater and coastal marine ecosystems: Ecological and  
 951 geochemical significance. *Limnology and Oceanography*, 33(4part2), 702–724.  
 952 <https://doi.org/10.4319/lo.1988.33.4part2.0702>
- 953 Silver S. & Phung L.T. (2005) A bacterial view of the periodic table: genes and proteins for toxic  
 954 inorganic ions. *Journal of Industrial Microbiology & Biotechnology*, **32**, 587-605.  
 955 <https://doi.org/10.1007/s10295-005-0019-6>
- 956 Skjelkvåle, B. L., & de Wit, H. A. (2011). Trends in precipitation chemistry, surface water chemistry  
 957 and aquatic biota in acidified areas in Europe and North America from 1990 to 2008 (ICP  
 958 Waters report 106/2011). In 126. Norsk institutt for vannforskning.  
 959 <https://niva.brage.unit.no/niva-xmlui/handle/11250/215591>
- 960 Skyllberg, U. (2008). Competition among thiols and inorganic sulfides and polysulfides for Hg and  
 961 MeHg in wetland soils and sediments under suboxic conditions: Illumination of controversies  
 962 and implications for MeHg net production. *Journal of Geophysical Research:*  
 963 *Biogeosciences*, 113(G2). <https://doi.org/10.1029/2008JG000745>
- 964 Sobek, S., Algesten, G., Bergström, A.-K., Jansson, M., & Tranvik, L. J. (2003). The catchment and  
 965 climate regulation of pCO<sub>2</sub> in boreal lakes. *Global Change Biology*, 9(4), 630–641.  
 966 <https://doi.org/10.1046/j.1365-2486.2003.00619.x>
- 967 Stumm W. & Morgan J.J. (1981) *Aquatic Chemistry. An introduction emphasizing chemical*  
 968 *equilibria in natural waters*, Wiley Interscience, New York.

- 969 Stumm, W., & Morgan, J. J. (1996). *Aquatic chemistry: Chemical equilibria and rates in natural*  
 970 *waters* (3rd ed.). Wiley.
- 971 Taipale S.J. & Sonninen E. (2009) The influence of preservation method and time on the delta C-13  
 972 value of dissolved inorganic carbon in water samples. *Rapid Communications in Mass*  
 973 *Spectrometry*, **23**, 2507-2510. <https://doi.org/10.1002/rcm.4072>
- 974 Takahashi H.A., Handa H., Sugiyama A., Matsushita M., Kondo M., Kimura H. & Tsujimura M.  
 975 (2019) Filtration and exposure to benzalkonium chloride or sodium chloride to preserve water  
 976 samples for dissolved inorganic carbon analysis. *Geochemical Journal*, **53**, 305-318.  
 977 <https://doi.org/10.2343/geochemj.2.0570>
- 978 Thottathil, S. D., Reis, P. C. J., & Prairie, Y. T. (2019). Methane oxidation kinetics in northern  
 979 freshwater lakes. *Biogeochemistry*, *143*(1), Article 1. [https://doi.org/10.1007/s10533-019-](https://doi.org/10.1007/s10533-019-00552-x)  
 980 [00552-x](https://doi.org/10.1007/s10533-019-00552-x)
- 981 Tipping E. (2007) Modelling the interactions of Hg(II) and methylmercury with humic substances  
 982 using WHAM/Model VI. *Applied Geochemistry*, **22**, 1624-1635.
- 983 Tørseth, K., Aas, W., Breivik, K., Fjæraa, A. M., Fiebig, M., Hjellbrekke, A. G., Lund Myhre, C.,  
 984 Solberg, S., & Yttri, K. E. (2012). Introduction to the European Monitoring and Evaluation  
 985 Programme (EMEP) and observed atmospheric composition change during  
 986 1972&ndash;2009. *Atmospheric Chemistry and Physics*, *12*(12), 5447–5481.  
 987 <https://doi.org/10.5194/acp-12-5447-2012>
- 988 Ullmann, F., Gerhartz, W., Yamamoto, Y. S., Campbell, F. T., Pfefferkorn, R., & Rounsaville, J. F.  
 989 (1985). Ullmann's encyclopedia of industrial chemistry (5th, completely rev. ed ed.). VCH.
- 990 UNESCO/IHA. (2008). *Assessment of the GHG status of freshwater reservoirs: Scoping paper*  
 991 (IHP/GHG-WG/3; p. 28). UNESCO/IHA, International Hydropower Association -  
 992 International Hydrological Programme, Working Group on Greenhouse Gas Status of  
 993 Freshwater Reservoirs. <https://unesdoc.unesco.org/ark:/48223/pf0000181713>
- 994 UNESCO/IHA. (2010). *GHG Measurement Guidelines for Freshwater Reservoirs* (p. 154).  
 995 UNESCO/IHA, International Hydropower Association.  
 996 [https://www.hydropower.org/publications/ghg-measurement-guidelines-for-freshwater-](https://www.hydropower.org/publications/ghg-measurement-guidelines-for-freshwater-reservoirs)  
 997 [reservoirs](https://www.hydropower.org/publications/ghg-measurement-guidelines-for-freshwater-reservoirs)
- 998 [Urabe, J., Iwata, T., Yagami, Y., Kato, E., Suzuki, T., Hino, S., & Ban, S. \(2011\). Within-lake and](#)  
 999 [watershed determinants of carbon dioxide in surface water: A comparative analysis of a](#)  
 1000 [variety of lakes in the Japanese Islands. \*Limnology and Oceanography\*, \*56\*\(1\), 49–60.](#)  
 1001 <https://doi.org/10.4319/lo.2011.56.1.0049>
- 1002 [Vachon, D., & Prairie, Y. T. \(2013\). The ecosystem size and shape dependence of gas transfer](#)  
 1003 [velocity versus wind speed relationships in lakes. \*Canadian Journal of Fisheries and Aquatic\*](#)  
 1004 [Sciences](#), *70*(12), Article 12. <https://doi.org/10.1139/cjfas-2013-0241>
- 1005 Valiente, N., Eiler, A., Alleesson, L., Andersen, T., Clayer, F., Crapart, C., Dörsch, P., Fontaine, L.,  
 1006 Heuschele, J., Vogt, R., Wei, J., de Wit, H. A., & Hessen, D. O. (2022). *Catchment properties*  
 1007 *as predictors of greenhouse gas concentrations across a gradient of boreal lakes.*  
 1008 *10*(880619). <https://doi.org/10.3389/fenvs.2022.880619>
- 1009 Valinia, S., Englund, G., Moldan, F., Futter, M. N., Köhler, S. J., Bishop, K., & Fölster, J. (2014).  
 1010 Assessing anthropogenic impact on boreal lakes with historical fish species distribution data  
 1011 and hydrogeochemical modeling. *Global Change Biology*, *20*(9), 2752–2764.  
 1012 <https://doi.org/10.1111/gcb.12527>
- 1013 van Grinsven, S., Oswald, K., Wehrli, B., Jegge, C., Zopfi, J., Lehmann, M. F., & Schubert, C. J.  
 1014 (2021). Methane oxidation in the waters of a humic-rich boreal lake stimulated by  
 1015 photosynthesis, nitrite, Fe(III) and humics. *Biogeosciences*, *18*(10), 3087–3101.  
 1016 <https://doi.org/10.5194/bg-18-3087-2021>
- 1017 Wanninkhof, R. (2014). Relationship between wind speed and gas exchange over the ocean revisited.  
 1018 *Limnology and Oceanography: Methods*, *12*(6), Article 6.  
 1019 <https://doi.org/10.4319/lom.2014.12.351>
- 1020 [Webb, J. R., Santos, I. R., Maher, D. T., Macdonald, B., Robson, B., Isaac, P., & McHugh, I. \(2018\).](#)  
 1021 [Terrestrial versus aquatic carbon fluxes in a subtropical agricultural floodplain over an annual](#)  
 1022 [cycle. \*Agricultural and Forest Meteorology\*, \*260–261\*, 262–272.](#)  
 1023 <https://doi.org/10.1016/j.agrformet.2018.06.015>

Formatted: English (United States)

- 1024 Weiss R.F. & Price B.A. (1980) Nitrous oxide solubility in water and seawater. *Marine Chemistry*, **8**,  
1025 347-359. [https://doi.org/10.1016/0304-4203\(80\)90024-9](https://doi.org/10.1016/0304-4203(80)90024-9)
- 1026 Weyhenmeyer, G. A., Hartmann, J., Hessen, D. O., Kopáček, J., Hejzlar, J., Jacquet, S., Hamilton, S.  
1027 K., Verburg, P., Leach, T. H., Schmid, M., Flaim, G., Nöges, T., Nöges, P., Wentzky, V. C.,  
1028 Rogora, M., Rusak, J. A., Kosten, S., Paterson, A. M., Teubner, K., ... Zechmeister, T.  
1029 (2019). Widespread diminishing anthropogenic effects on calcium in freshwaters. *Scientific*  
1030 *Reports*, 9(1), Article 1. <https://doi.org/10.1038/s41598-019-46838-w>
- 1031 Wilhelm E., Battino R. & Wilcock R.J. (1977) Low-pressure solubility of gases in liquid water.  
1032 *Chemical Reviews*, **77**, 219-262. <https://doi.org/10.1021/cr60306a003>
- 1033 Wilson J., Munizzi J. & Erhardt A.M. (2020) Preservation methods for the isotopic composition of  
1034 dissolved carbon species in non-ideal conditions. *Rapid Communications in Mass*  
1035 *Spectrometry*, **34**. <https://doi.org/10.1002/rcm.8903>
- 1036 Xiao, S., Yang, H., Liu, D., Zhang, C., Lei, D., Wang, Y., Peng, F., Li, Y., Wang, C., Li, X., Wu, G.,  
1037 & Liu, L. (2014). Gas transfer velocities of methane and carbon dioxide in a subtropical  
1038 shallow pond. *Tellus B: Chemical and Physical Meteorology*, 66(1), 23795.  
1039 <https://doi.org/10.3402/tellusb.v66.23795>
- 1040 Xu F.F. & Imlay J.A. (2012) Silver(I), Mercury(II), Cadmium(II), and Zinc(II) Target Exposed  
1041 Enzymic Iron-Sulfur Clusters when They Toxify Escherichia coli. *Applied and Environmental*  
1042 *Microbiology*, **78**, 3614-3621. <https://doi.org/10.1128/aem.07368-11>
- 1043 Yamamoto S., Alcauskas J.B. & Crozier T.E. (1976) Solubility of methane in distilled water and  
1044 seawater. *Journal of Chemical and Engineering Data*, **21**, 78-80.  
1045 <https://doi.org/10.1021/jc60068a029>
- 1046 Yan, F., Sillanpää, M., Kang, S., Aho, K. S., Qu, B., Wei, D., Li, X., Li, C., & Raymond, P. A.  
1047 (2018). Lakes on the Tibetan Plateau as Conduits of Greenhouse Gases to the Atmosphere.  
1048 *Journal of Geophysical Research: Biogeosciences*, 123(7), 2091–2103.  
1049 <https://doi.org/10.1029/2017JG004379>
- 1050 Yang H., Andersen T., Dorsch P., Tominaga K., Thrane J.E. & Hessen D.O. (2015) Greenhouse gas  
1051 metabolism in Nordic boreal lakes. *Biogeochemistry*, **126**, 211-225.  
1052 <https://doi.org/10.1007/s10533-015-0154-8>
- 1053